

Bootstrapping Lieb-Schultz-Mattis anomalies

Ryan A. Lanzetta  and Lukasz Fidkowski

Department of Physics, University of Washington, Seattle, Washington 98195, USA

 (Received 24 August 2022; revised 20 April 2023; accepted 20 April 2023; published 19 May 2023)

We incorporate the microscopic assumptions that lead to a certain generalization of the Lieb-Schultz-Mattis (LSM) theorem for one-dimensional spin chains into the conformal bootstrap. Our approach accounts for the “LSM anomaly” possessed by these spin chains through a combination of modular bootstrap and correlator bootstrap of symmetry defect operators. Specifically, we obtain universal bounds on the local operator content of $(1+1)d$ conformal field theories (CFTs) that could describe translationally invariant lattice Hamiltonians with a $\mathbb{Z}_N \times \mathbb{Z}_N$ symmetry realized projectively at each site. We assume, for such models, that in the CFT the lattice translation symmetry is realized as an emanant internal \mathbb{Z}_N symmetry. We present bounds on local operators both with and without refinement by their global symmetry representations. Interestingly, we can obtain nontrivial bounds on charged operators when N is odd, which turns out to be impossible with modular bootstrap alone. Our bounds exhibit distinctive kinks, some of which are approximately saturated by known theories and others that are unexplained. We discuss additional scenarios with the properties necessary for our bounds to apply, including certain multicritical points between $(1+1)d$ symmetry protected topological phases, where we argue that the anomaly studied in our bootstrap calculations should emerge.

DOI: [10.1103/PhysRevB.107.205137](https://doi.org/10.1103/PhysRevB.107.205137)

I. INTRODUCTION

A. Overview

Identifying the low-energy spectrum of a given lattice Hamiltonian is an important goal of quantum many-body theory. In certain cases, depending on the symmetries of the model, the qualitative nature of its spectrum can be constrained, thus restricting the potential quantum field theory (QFT) descriptions. A famous and powerful result of this kind, known as the Lieb-Schultz-Mattis (LSM) theorem, is that half-odd-integer spin Heisenberg chains are gapless [1]. This is to be contrasted with the Haldane gap for the case of integer spin [2,3]. Following these results, various generalizations in similar spirit have been made: in higher dimensions [4,5], with more generic spatial symmetries [6–9], including the magnetic translation group [10–12], and with higher form symmetries [13]. In this paper, we will be concerned with an extension of the LSM theorem involving translations to general global symmetry groups, where it is expected that a translationally invariant local spin chain with an on-site global symmetry represented projectively at each site cannot be trivially gapped [14–17]. This leaves gaplessness or spontaneous symmetry breaking (SSB) as the only possibilities in one spatial dimension.

The modern formulation of LSM-type theorems is in terms of ’t Hooft anomalies [18–22], which can be viewed as obstructions to gauging a global symmetry. For a lattice model subject to the generalized translation LSM theorem with an internal symmetry G , what we will refer to as the *LSM anomaly* is a mixed anomaly between lattice translation symmetry and G . This anomaly arises due to the fact that inserting a defect of translation symmetry amounts to adding one site, which carries a projective representation of G . Thus, in the presence of such translation symmetry defects, it is not possible to

gauge G . This ’t Hooft anomaly must be matched by both the lattice and continuum QFT descriptions [23], making it a powerful nonperturbative tool to aid in identifying candidate low-energy theories—typically a complicated task. More general anomalies in bosonic lattice models have been studied throughout the literature, see e.g., [24–27].

Field theory descriptions of lattice models will generally possess a different set of symmetries, whose relation to the lattice symmetries is constrained by requiring the existence of a group homomorphism relation $\gamma : G_{\text{UV}} \rightarrow G_{\text{IR}}$ that specifies how the lattice symmetries are realized at low energy. The homomorphism γ must also be compatible with anomaly matching, in a sense that we will describe. In this paper, we will consider $G_{\text{UV}} = \mathbb{Z}^{\text{trans}} \times \mathbb{Z}_N^2$ on an infinite lattice, which describes systems with translation symmetry and an internal \mathbb{Z}_N^2 symmetry. In the context of LSM, we assume that the lattice translation symmetry is realized as an *emanant* (in the sense of [28]) \mathbb{Z}_N internal symmetry in the CFT description of the system, leading the CFTs we consider to have a minimal, internal symmetry group $G = \mathbb{Z}_N^3$. An emanant symmetry of a low-energy theory is one for which any operator that breaks it also breaks the microscopic symmetry from which it emanates. We note that \mathbb{Z}_N is not the only possible such emanant symmetry, as we will discuss briefly later on, but we restrict our study to this case for simplicity and since it is realized in various relevant microscopic models and their field-theoretic descriptions [18,29]. Note that for the remainder of the paper we will refer to the particular continuum manifestations of these anomalies that we study as LSM anomalies, although in the continuum context they are anomalies of purely internal symmetries and do not have to arise out of lattice models with mixed anomalies between spatial and internal symmetries. Indeed, we will also discuss a scenario where the same \mathbb{Z}_N^3 mixed anomalies in the field theory description are emergent

(that is, a microscopic \mathbb{Z}_N^2 internal symmetry is assumed and the third \mathbb{Z}_N is emergent and has a mixed anomaly with the microscopic symmetry), in the context multicritical points of symmetry protected topological (SPT) phases, where no LSM constraint is expected.

Within the realm of QFT, another set of nonperturbative techniques are those related to conformal field theory (CFT), among them being the numerical conformal bootstrap. Following recent work combining \mathbb{Z}_N symmetries and anomalies with modular bootstrap [30,31], in this paper we will use conformal bootstrap to bound the space of CFTs that possess the aforementioned continuum versions of certain LSM anomalies arising in lattice models with global, internal symmetry $G_{\text{int}} = \mathbb{Z}_N^2$. Fully incorporating the signatures of these LSM anomalies into bootstrap is somewhat subtle; to do so, we introduce a technique that augments modular bootstrap by incorporating additional numerical bounds that come from imposing crossing symmetry on four-point functions of certain symmetry defect operators. This approach allows us to obtain universal bounds on the local operator content of $(1+1)d$ CFTs in a way that is refined by LSM anomalies.

B. Background, methods, and motivation

Lattice models with the kinds of symmetries and anomalies we have mentioned have received some recent attention, partially motivating this paper. Under the assumption of a unique ground state, CFTs naturally describe gapless spin chains satisfying LSM constraints, since any scale-invariant, $(1+1)d$ QFT is necessarily a CFT, under mild assumptions [32–35]. Indeed, in some recent numerical simulation work it was observed that entire stable, gapless phases of translation-invariant spin chains, subject to LSM constraints with on-site $\mathbb{Z}_N \times \mathbb{Z}_N$ symmetries, are effectively described by theories within the conformal manifolds of $N-1$ compact bosons for $N=2, 3$ [29]. It was argued in Ref. [29] that a similar compact boson description should be valid for arbitrary, odd N . Further, the authors of Ref. [29] suggest that the central charge $c = N-1$ of the compact boson theories may be the minimum necessary to accommodate the LSM anomaly when the only microscopically-imposed symmetry is \mathbb{Z}_N^3 , assuming that the $\mathbb{Z}_{\text{trans}}$ is realized as \mathbb{Z}_N in the low-energy global symmetry group G_{IR} . As noted by Ref. [36], which also contains some discussion of the LSM anomalies studied in this paper, if one imposes instead a larger $PSU(N)$ internal symmetry, which is apparently emergent in a subset of the models studied by Ref. [29], then this minimum central charge is indeed $c = N-1$ by the Sugawara construction [37]. However, as we will point out, there are trivial counterexamples to this bound when the minimum symmetry imposed at low energy is \mathbb{Z}_N^3 and N is a product of coprime integers. Nonetheless, with a suitable quantitative modification to the possible central charge bound in these cases, there persists the difficult problem of determining whether nontrivial counterexamples exist. Thus, one of the goals of this paper will be to look for bootstrap signatures of potential theories with a lower central charge that could have the LSM anomalies.

One possible explanation for the lack of counterexamples to the suggested central charge bound is that the space of $(1+1)d$ CFTs with $c > 1$ remains largely uncharted terri-

tory. Unlike for $c < 1$, where all unitary theories are known [38,39], most explicit constructions of compact, unitary CFTs with $c > 1$ are rational CFTs [40] (RCFTs) with enhanced symmetry or coupled free bosons. Resurrecting ideas used originally to exactly solve many of the known examples of $(1+1)d$ CFTs, in the past several years it was realized that instead of attempting full solutions of specific CFTs, a still powerful and more tractable goal is to attempt to rule out, using numerical optimization techniques such as linear or semidefinite programming, certain regions in the space of all possible CFTs [41–43]—this represents the modern, numerical conformal bootstrap program. This is possible due to unitarity and other more stringent mathematical consistency requirements inherent to CFTs. In general dimensions, the main consistency requirement is the crossing symmetry of four-point functions. Within numerical bootstrap, one can attempt to show that certain assumptions about the spectrum of a CFT can lead to incompatibility with crossing symmetry. This approach, termed *correlator bootstrap*, has had much success, and in some cases has gone so far as to produce numerical solutions to certain theories, as has been done in the case of the $3d$ Ising CFT [42,44,45]. These advances have especially been made possible following the introduction of specialized semidefinite programming packages for conformal bootstrap applications such as SDPB [46].

In the setting of $(1+1)d$ CFTs, the possible constraints on the CFT data are more powerful than in $d > 2$ due to the correspondence between the local primary operator spectrum and the decomposition of the torus partition function into Virasoro characters, which is subject to modular invariance. Both analytically and numerically, it was shown that imposing modular invariance of the partition function gives generic bounds on the operator content of a unitary, compact, bosonic $(1+1)d$ CFT, guaranteeing, for instance, an upper bound on the scaling dimension of the lightest primary field for any CFT [47,48]. This should be contrasted with correlator bootstrap, where to obtain any bounds one must typically make an additional assumption that the theory possesses some fields with a particular scaling dimension [49]. This approach, termed *modular bootstrap*, has also been generalized to bosonic, $(1+1)d$ CFTs with anomalous and nonanomalous \mathbb{Z}_N global symmetries by imposing modular covariance of the torus partition function twisted by symmetry defects [30,31], as we mentioned. Additional progress in a similar vein has been made for fermionic CFTs with nonanomalous and anomalous global symmetries [50–52], but in this paper we will focus on bosonic theories.

The \mathbb{Z}_N anomalies studied in previous modular bootstrap works are characterized by anomalous spin selection rules for so-called defect operators hosted at the end of topological defect lines (TDLs) implementing the \mathbb{Z}_N symmetry [53]. These spin constraints lead to stronger unitarity bounds on the scaling dimensions for such operators. From these inputs emerges the general result that anomalous \mathbb{Z}_N symmetries are necessarily accompanied by charged degrees of freedom at low energy. Further, the bounds on \mathbb{Z}_N -symmetric operators depend strongly on the anomaly. However, more complicated symmetry groups may have more complicated anomalies with more subtle signatures, ones that even do not include anomalous defect spin-selection rules. A \mathbb{Z}_N^3 symmetry with the

aforementioned LSM anomaly is one case where this scenario can occur. As already alluded to, the main distinguishing signature of the LSM anomaly is that symmetry defect operators of one \mathbb{Z}_N subgroup transform in a projective representation of the remaining \mathbb{Z}_N^2 subgroup. Crucially, when N is odd, this is essentially the only signature of the LSM anomaly; in these cases, there are no nontrivial defect spin selection rules, so modular bootstrap by itself is insensitive to the LSM anomaly and, thus, cannot give a bound on charged operators. On the other hand, our approach gives rather tight bounds on charged operators at low central charge and uncovers various intriguing kinks.

To incorporate the LSM anomalies into bootstrap, we augment modular bootstrap by incorporating certain bounds coming from correlator bootstrap. Our approach exploits the constraining power of both crossing symmetry of defect operators and modular covariance of the twisted partition function as follows. Suppose we are trying to rule out some gap in the spectrum of scaling dimensions of local operators for CFTs with a particular central charge. In the case of the \mathbb{Z}_N modular bootstrap, the presence of an anomaly sets *universal* lower bounds on the scaling dimension of any \mathbb{Z}_N symmetry defect operator; for the LSM anomaly, we derive a nonuniversal lower bound that depends on the assumed gap in the local operator spectrum and, in some cases, the central charge. The reason for this lower bound is that taking the operator product expansion (OPE) of light defect operators can produce light local operators; precisely how light the defect operators can be without necessarily producing a local operator whose scaling dimension violates the assumed gap in the local operator spectrum is quantified using correlator bootstrap. Additionally, in some cases the gaps in the spectrum of local and defect operators further lead to a lower bound on the central charge. This provides yet another route to improve our lower bound on the scaling dimension of the lightest defect operator, since the lower bound on the central charge must not be higher than the assumed central charge. On the other hand, for modular covariance of the twisted partition function to be obeyed, the lightest local operator and the lightest defect operator typically cannot both be too heavy; in particular, if the gap in the spectrum of local operators is large—for instance, a gap that we are trying to rule out—there often exists an upper bound on the gap in the spectrum of defect operators. This reasoning applies even when the gap among local operators is assumed to exist only in the charged sector, or only in the neutral sector. Modular bootstrap thus has the potential to rule out the combined gaps in the local and defect operator spectra, where the latter gap is implied by the former, leading to a contradiction and allowing us to rule out the assumed gap in the local operator spectrum.

Our main results, shown in Figs. 1 and 2, are upper bounds, as a function of central charge c , on the lightest local operators with various symmetry properties for CFTs saturating the \mathbb{Z}_N^3 LSM anomaly for $N = 2, 3, 4, 5, 6$. These bounds can be thought of as a refinement of the more qualitative LSM-type theorems, which only exclude a nondegenerate gapped ground state. Our results, by contrast, state that, for CFTs saturating the LSM anomalies, not only must there exist charged states with energies $\mathcal{O}(1/L)$ (in a ring geometry with periodic boundary conditions with L the circumference and under the

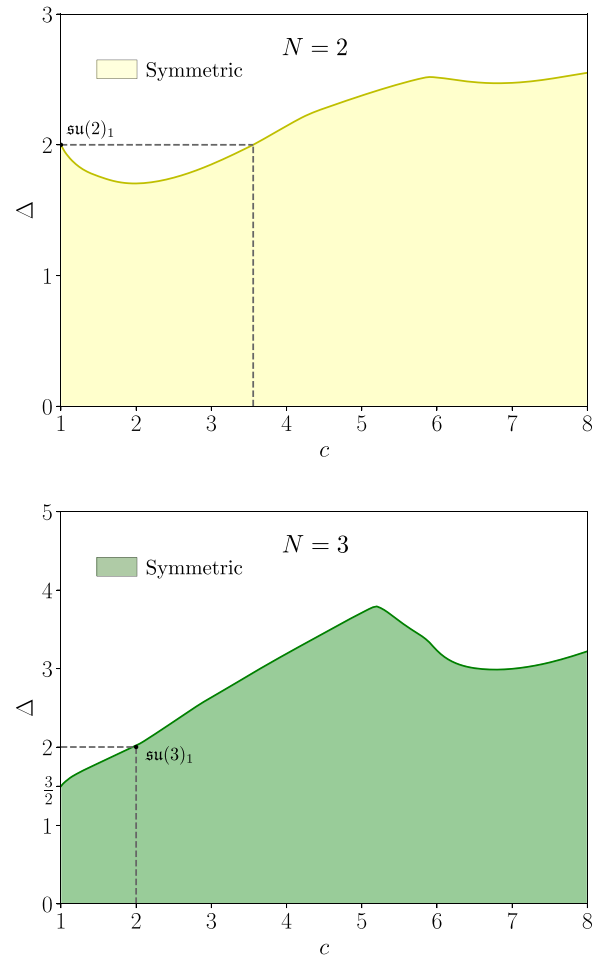


FIG. 1. Upper bounds on the scaling dimension of the lightest \mathbb{Z}_N^3 -symmetric scalar operator in a theory with the LSM anomaly, as a function of central charge, for $N = 2, 3$. The shaded region in each plot is thus the allowed region for the lightest symmetric, scalar operator. In obtaining these bounds, we did not make use of the additional improvements to standard modular bootstrap with global symmetry that we introduce in this paper. The bounds were computed with $\Lambda^{\text{mod}} = 25$ and $S_{\text{max}}^{\text{mod}} = 50$ (see Sec. IV for implementation details).

assumption of a unique ground state), but there is also a precise upper bound $\sim \Delta(c)/L$ on the energy of such states when the lattice model is described at low energy by a CFT with central charge c . There are various additional microscopic realizations of lattice models that can be described by the kinds of CFTs we put bounds on. These include certain multicritical points of $(1+1)d$ symmetry protected topological (SPT) phases and edge theories of certain $(2+1)d$ SPT phases.

C. Organization

The structure of the remainder of this paper is as follows. In Sec. II we will present our universal bootstrap bounds on the local operator spectrum of $(1+1)d$ CFTs with the \mathbb{Z}_N^3 LSM anomalies for various N , and further discuss the implications of our bounds to the theory of multicritical points of SPT phase transitions. In Sec. III we will provide technical background regarding symmetries and anomalies in $(1+1)d$

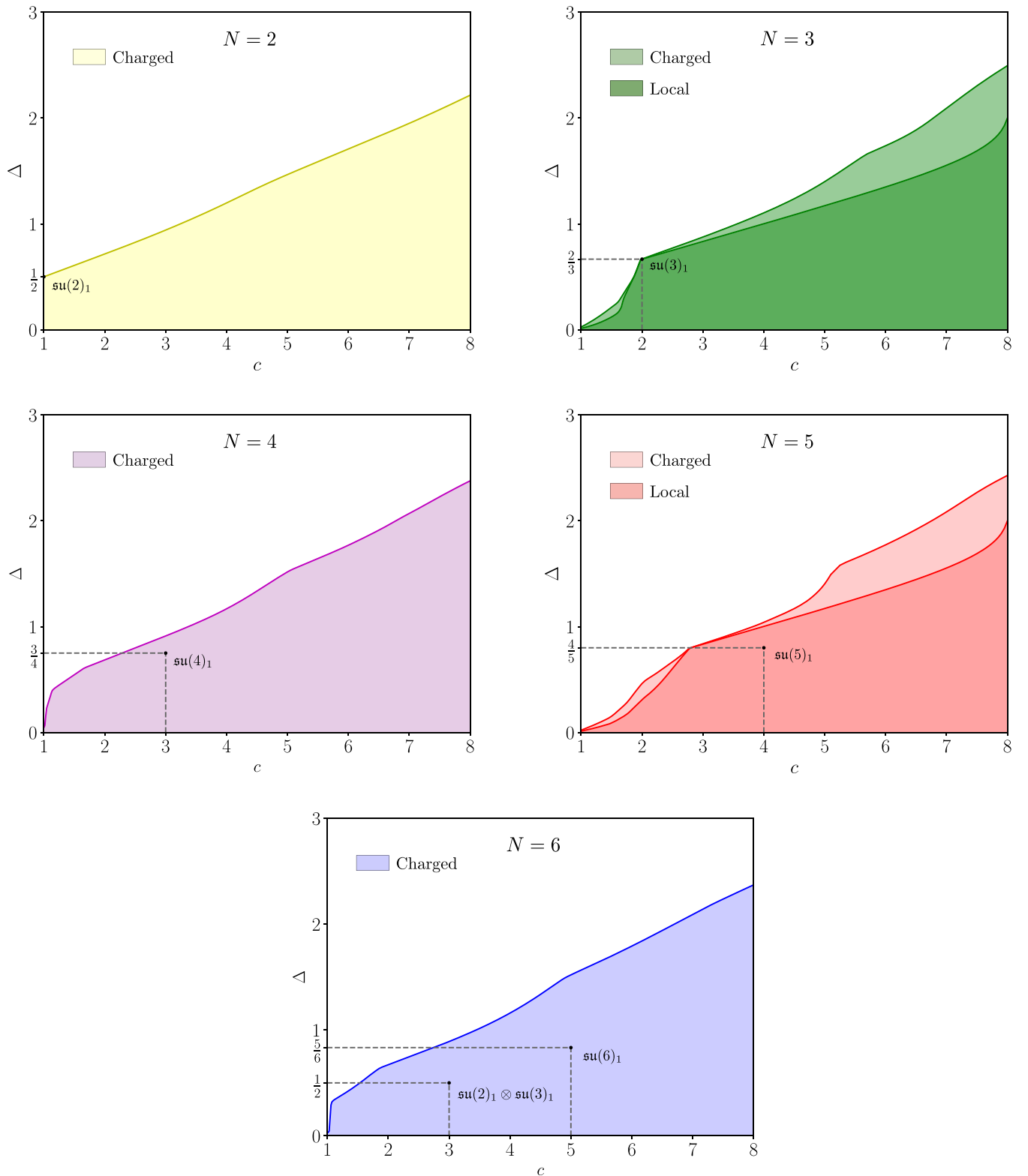


FIG. 2. Two kinds of universal upper bounds on the scaling dimension of local operators. For $N = 2, \dots, 6$, we find an upper bound on the scaling dimension of the lightest charged, scalar operator, where a charged operator is any operator transforming in a nontrivial representation of \mathbb{Z}_N^3 . For $N = 3, 5$, we additionally obtain a stronger bound on the lightest local operator, irrespective of its symmetry properties. The shaded regions represent the allowed regions for the scaling dimensions of such operators in each of the aforementioned cases. The bounds shown here make full use of our improvements to modular bootstrap with global symmetries and anomalies and were computed with $\Lambda^{\text{mod}} = 25$ and $S_{\text{max}}^{\text{mod}} = 50$ (see Sec. IV for implementation details).

CFT, including details about the TDL formalism and how the LSM anomalies manifest within it. Then in Sec. IV we will explain aspects of our numerical bootstrap approach and additionally present some of the other numerical bounds (Figs. 9 and 10, see below) that went into our final calculations. Finally, in Sec. V we will make closing remarks and discuss potential future avenues for research. We provide additionally an Appendix with details about our modular bootstrap calculations.

II. MAIN RESULTS

Here we present our main results, which include universal numerical bootstrap bounds on the local primary operator spectrum of unitary, compact $(1 + 1)d$ CFTs with a \mathbb{Z}_N^3 symmetry and LSM anomaly. We further discuss an application of our numerical bounds to the theory of phase transitions between symmetry protected topological (SPT) phases. The precise details of the LSM anomaly and its implications on the structure of the theories that saturate it will be discussed later. We do not study theories with $c < 1$ since it is known that the unitary models cannot possess the kinds of symmetries, let alone anomalies, that we study in this paper [54].

We obtain three types of numerical bounds, each of which will be an upper bound on the scaling dimension of the lightest scalar primary field transforming in some representation of \mathbb{Z}_N^3 . The three possibilities we consider for the representations of operators are the trivial representation, any nontrivial representation, or any representation. The first two cases then are upper bounds on the scaling dimension of the lightest symmetric or charged scalar local primary, respectively, and the last case represents an upper bound on the lightest local, scalar operator. We only present bounds on the lightest \mathbb{Z}_N^3 -symmetric operator for $N = 2, 3$, since for larger N the bounds converge very slowly, and the improvements introduced in this paper do not improve our ability to guarantee relevant, symmetric, scalar operators.

Before discussing our bounds, we mention that examples of CFTs with the properties necessary for our bootstrap bounds to apply have been discussed, with emphasis on their LSM anomalies, in Ref. [29]. As mentioned, the main class of examples for theories with the \mathbb{Z}_N^3 LSM anomalies may be found within the conformal manifolds of $N - 1$ compact bosons with certain symmetry constraints. However, we also remark that it is possible to find examples of theories with these LSM anomalies with lower central charge than what is suggested in Ref. [29]. When $N = \prod_i n_i$ with n_i all co-prime integers, CFTs with the $N = \prod_i n_i$ LSM anomaly can be constructed by taking the tensor product of theories with the LSM anomaly corresponding to each n_i . The reason for this is that in this situation $\mathbb{Z}_N = \bigoplus_i \mathbb{Z}_{n_i}$. It can be checked straightforwardly that projective representations of \mathbb{Z}_N^2 can be decomposed into tensor products of the projective representations of $\mathbb{Z}_{n_i}^2$ and further that the other properties implied by the LSM anomaly corresponding to N , such as the spin selection rules of defect operators (see Sec. III and Table I), are the same. Using, for instance, the WZW models $\mathfrak{su}(n_i)_1$, we can thus construct theories with the $N = \prod_i n_i$ LSM anomaly that have central charge $c = \sum_i (n_i - 1) < N - 1$.

TABLE I. The values k of \mathbb{Z}_M anomalies appearing in (11) for elements of the groups \mathbb{Z}_N^3 for theories with the LSM anomaly, i.e., when the full cocycle is given by (14). The columns are organized by the order of the elements $g = (g_1, g_2, g_3) \in \mathbb{Z}_N^3$, and the rows each correspond to a different choice of N .

N	Order of $g \in G$				
	2	3	4	5	6
2	1 if $g = (1, 1, 1)$ 0 else				
3		0			
4	0		2 if g_i odd 0 else		
5				0	
6	1 if $g = (3, 3, 3)$ 0 else	0			3 if g_i odd 0 else

A. Universal bounds on lightest \mathbb{Z}_N^3 -symmetric scalar

Here we discuss our bounds on the lightest \mathbb{Z}_N^3 -symmetric scalar operator for $N = 2, 3$, which are shown in Fig. 1. Bounds on symmetric, scalar operators are interesting primarily to determine whether theories whose central charge is within a certain range *cannot* describe stable gapless phases where the microscopically-imposed symmetry is \mathbb{Z}_N^3 . In the presence of such a symmetry-preserving relevant operator, an RG flow may be triggered to a nearby phase with the same symmetry, but due to the anomaly this flow will generally lead either to a phase where the symmetry is spontaneously broken, or perhaps the flow will end at a nontrivial CFT fixed point. In either case, the initial CFT is thus unstable. The calculations performed in this section involve only the standard modular bootstrap setup with global symmetries and \mathbb{Z}_N anomalies of Refs. [30,31], with slight modification to include the larger symmetry group. It turns out that our improvements to this setup, which we use in the remainder of our calculations, do not lead to an enlargement of the range of values of central charge where a relevant symmetric scalar is guaranteed. This trend continues for larger N , where our methods do not lead to any nontrivial range of values of the central charge for which a relevant, \mathbb{Z}_N^3 -symmetric operator is guaranteed.

1. $N = 2$

For $N = 2$, modular bootstrap is somewhat sensitive to the LSM anomaly since it sees that one of the \mathbb{Z}_2 TDLs is anomalous (see Table I). Our bound leads to a range of values of central charge such that any theory in the range with the $N = 2$ LSM anomaly must contain a relevant, \mathbb{Z}_2^3 -symmetric scalar operator. The range is approximately

$$1 < c < 3.5565.$$

Our bound is saturated at $c = 1$ by $\mathfrak{su}(2)_1$, whose lightest operator symmetric under \mathbb{Z}_2^3 is exactly marginal with $\Delta = 2$.

2. $N = 3$

In this case, we see that any CFT with a nonanomalous \mathbb{Z}_3^3 symmetry (or, equivalently for the calculations presented here, a \mathbb{Z}_3^3 symmetry with the LSM anomaly) must have a

relevant symmetric scalar if its central charge is $c < 2$. The WZW model $\mathfrak{su}(3)_1$ nearly saturates our bound at $c = 2$, whose lightest operator \mathbb{Z}_3 -symmetric is exactly marginal. In Ref. [31], it was shown also that when $c < 2$ a \mathbb{Z}_3 -symmetric, relevant, scalar operator must be present. The analogous bounds for \mathbb{Z}_3^3 cannot be stronger than this bound, since imposing more symmetry can only make it harder for a given operator to remain symmetric, so it is interesting that our \mathbb{Z}_3^3 bound is still powerful enough to guarantee relevant operators in this range of central charge.

B. Universal bounds on lightest \mathbb{Z}_N^3 -charged scalar

We now discuss our bounds on the lightest \mathbb{Z}_N^3 charged operator, which are shown in Fig. 2. We define a \mathbb{Z}_N^3 -charged operator as a local operator transforming in any nontrivial representation of \mathbb{Z}_N^3 . For odd, prime N , this choice loses no generality since all nontrivial representations are equivalent in the sense that they are related by outer automorphisms, i.e., a relabeling of the group elements. This relabeling is allowed since each \mathbb{Z}_N TDL for a given N has the same spin-selection rule (see Sec. III and Appendix). For even N , there are different classes of representations, so in principle more refined bounds could be obtained by bounding the lightest operator in each class separately but, for simplicity, we will not present such bounds.

1. $N = 2$

Our $N = 2$ bound does not contain many features. The known theories with minimal central charge and the $N = 2$ LSM anomaly are the $c = 1$ compact boson theories on the circle branch. The theory that maximizes the gap in the \mathbb{Z}_2^3 -charged operator spectrum is the WZW model $\mathfrak{su}(2)_1$, whose lightest charged, scalar operator has scaling dimension $\Delta = \frac{1}{2}$.

2. $N = 3$

Our bound on the lightest charged operator for $N = 3$ has various interesting features. First of all, the bound approaches $\Delta=0$ as $c \rightarrow 1$, which is in agreement with the analytical analysis of $c = 1$ theories that no such theory can have the LSM anomaly for $N=3$. This is quite striking in modular bootstrap calculations, which typically are not quite so strong, and is a feature shared by our bounds for other choices of $N>2$. The most obvious feature is that the $\mathfrak{su}(3)_1$ WZW CFT, which is the principal example of a WZW CFT with the $N = 3$ LSM anomaly, sits at a prominent kink of our upper bound. The $\mathfrak{su}(3)_1$ theory has $c = 2$ and its lightest charged scalar has scaling dimension $\Delta = \frac{2}{3}$.

We stress that in this case, since N is odd, modular bootstrap alone does not give a bound at all on the lightest charged operator since all \mathbb{Z}_3 subgroups, in this case, have no \mathbb{Z}_3 anomaly.

3. $N = 4$

This bound displays a few kink-like features at low values of the central charge that we cannot, at present, explain. The $c = 3$ compact boson theories are the only theories we know of with the $N = 4$ LSM anomaly, among which is the

WZW model $\mathfrak{su}(4)_1$. It is expected that $\mathfrak{su}(4)_1$ maximizes the scalar gap among the toroidal compactification CFTs at $c = 3$ [55,56]. (Maximizing the scalar gap in the moduli space of such theories at generic integral c is a difficult problem. See additionally Ref. [57] for interesting work related to this.) However, the question of which CFT absolutely maximizes the scalar gap at $c = 3$ remains an interesting puzzle; the universal upper bound on the scalar gap calculated in Ref. [48] is not saturated by $\mathfrak{su}(4)_1$ at $c = 3$. Consequently, we do not know whether there is any $c = 3$ theory that saturates our even larger upper bound on the lightest \mathbb{Z}_4^3 charged operator for theories with the $N = 4$ LSM anomaly.

4. $N = 5$

This bound is similar to the bound for $N = 3$ since again modular bootstrap alone gives no bound. Below $c = 4$, which is the minimal central charge we know of where theories with the $N = 5$ LSM anomaly are known to exist, we see two features that resemble kinks. The first occurs at $c \approx 2$ and is somewhat soft. Our upper bound at $c = 2$ is approximately equal to $\Delta = 0.462$. At this time we are not aware of any evidence to suggest that this corresponds to an actual theory, so it will be interesting to study this feature in future work. The second kink is more sharply defined and is somewhat more intriguing. The location of this kink, according to our plot in Fig. 2, which was computed with derivative orders $\Lambda^{\text{mod}} = \Lambda^{\text{cor}} = 25$ (for an explanation of the parameters describing our computational setup, see Sec. IV), is almost exactly at $c = \frac{14}{5}$, where our upper bound is equal to $\Delta = 0.8006$. This puts the WZW model $(\mathfrak{g}_2)_1$ essentially right at the location of this kink. However, as we discuss in the next subsection, we were able to rule out $(\mathfrak{g}_2)_1$ from having the $N = 5$ LSM anomaly with a more intensive calculation, so the origin of this kink remains a mystery.

At $c = 4$, the WZW CFT $\mathfrak{su}(5)_1$ is well within the allowed region, but as was the case with $N = 4$ we are not sure of a systematic way to maximize the scalar gap among the $c = 4$ compact boson theories, subject to the appropriate symmetry requirements, let alone among all CFTs, to see whether ultimately our bound is saturated by an actual CFT. Using the formalism developed in Refs. [56,58] seems like a promising approach, but we leave this interesting exercise to future work.

5. $N = 6$

This bound resembles closely our bound for $N = 4$, where we see some unexplained features at relatively low central charge. This is the first case where N is a product of coprime integers, so we can realize theories with the $N = 6$ LSM anomaly by taking the tensor product of any $N = 2$ theory with a $N = 3$ theory. Thus, using our currently known examples, we can produce theories with central charge equal to either $c = 3$ or $c = 5$ by taking the corresponding number of compact bosons and imposing the appropriate symmetries. Examples of WZW models (or tensor products thereof) in this category include $\mathfrak{su}(2)_1 \otimes \mathfrak{su}(3)_1$ and $\mathfrak{su}(6)_1$. Our analysis here is limited again by the issues we mentioned for $N = 4, 5$, and the WZW models we mentioned are even farther from achieving saturation with our bounds.

C. Universal bounds on lightest local scalar

As we are especially interested in finding numerical evidence for CFTs with the \mathbb{Z}_N^3 LSM anomaly with $c < N - 1$ for odd N , to which the suggested lower bound in Ref. [29] applies, we additionally obtain bounds on the lightest local operator transforming in any representation of \mathbb{Z}_N^3 . This is the strongest gap assumption we can make, while still being universal, and thus gives, numerically, the strongest bounds. We thus expect any features corresponding to actual theories to have the most clarity within these bounds. To obtain these bounds, we incorporate the correlator bootstrap lower bounds on central charge from Fig. 10 in addition to the bounds on scaling dimension from Fig. 9. This leads to a notable improvement of our bounds at relatively low central charge; we note that the stronger gap assumption within modular bootstrap alone did not lead to a significant difference in the resulting bounds.

1. $N = 3$

As expected, the theory $\mathfrak{su}(3)_1$ continues to lie at the $c = 2$ kink of this bound, which is sharpened further by the stronger assumptions placed on the operator content. Interestingly, at $c \approx 1.7$ it appears that another feature emerges. However, this feature does not take a sharper shape upon using more derivatives in the linear functional within modular bootstrap, as our bounds are very close to saturation in this range of central charge. The question of whether or not this feature is due to an actual CFT is left open. Above $c = 2$, our bound converges to the bound on the lightest scalar operator in any CFT obtained in Ref. [48].

2. $N = 5$

The feature present at $c \approx 2$ in the bound on the lightest charged scalar did not survive the stronger assumptions used to obtain this bound. Thus, if that feature is due to an operator in an actual CFT with the $N = 5$ LSM anomaly, this operator would have to be symmetric under the \mathbb{Z}_5^3 symmetry that carries the anomaly.

Similarly to the $N = 3$ case, the stronger assumptions used to obtain this bound sharpen the kink near $c = 2.8$ and, for the size of the functional used in making the $N = 5$ plot of Fig. 2, the theory $(\mathfrak{g}_2)_1$ is not yet ruled out. However, we also did a calculation where we improved some of our parameters to $\Lambda^{\text{mod}} = 41$ and $S_{\text{max}}^{\text{mod}} = 80$. Our bound at $\Lambda^{\text{mod}} = 25$ is very close to saturation in this range of central charge, but nonetheless we obtained an upper bound of $\Delta = 0.79990$ at $c = 2.8$, thus ruling out $(\mathfrak{g}_2)_1$. Studying this kink further is an interesting task we leave to future work. Even though we have not yet exactly pinned down the location of the kink, it seems a strong possibility that, in this case, we have uncovered evidence for a nontrivial example of some theory with the $N = 5$ LSM anomaly that has $c < 4$.

D. Application to multicritical points of $(1+1)d$ symmetry protected topological phases

Symmetry protected topological (SPT) phases are a special class of gapped Hamiltonians with a global symmetry G . When placed on a manifold without boundary, SPT phases

possess a unique, G -symmetric ground state that cannot be connected to a trivial product state by applying a finite depth local unitary circuit (FDLUC), where the local unitaries in the circuit individually preserve the global symmetry [59]. In one spatial dimension, SPT phases protected by a symmetry group G are classified by the group cohomology group $H^2(G, U(1))$. The group cohomology group encodes the algebraic structure of the phases under stacking, which is determined by its group multiplication [60]. Further, the class $[\alpha] \in H^2(G, U(1))$ labeling each phase determines the projective representation carried at each boundary endpoint when a Hamiltonian in a nontrivial SPT phase is placed on a lattice with a boundary.

An interesting area of study is that of the nature of second-order phase transitions between SPTs [61–64]. It has been argued by Bultinck [65] that for any SPT phase $[\alpha]$ satisfying the property that two copies of it is in the trivial SPT phase, i.e., $[\alpha]^2 = [1]$, any critical point describing a second-order phase transition between $[1]$ and $[\alpha]$ will have an emergent \mathbb{Z}_2 symmetry having a mixed anomaly with the internal symmetry G of the neighboring SPT phases. The mixed anomaly is given by a type-III cocycle $\omega \in H^1[\mathbb{Z}_2, H^2(G, U(1))] \subset H^3(\mathbb{Z}_2 \times G, U(1))$, which has the interpretation, in CFT language, that a defect operator of the emergent \mathbb{Z}_2 symmetry carries a projective representation of G .

We can roughly sketch the argument for the emergent symmetry and anomaly as follows. A key feature of an SPT Hamiltonian is that there is a FDLUC \mathcal{U} building its ground state from a trivial product state. Importantly, a FDLUC preserves the correlation length.

Now, consider a one-parameter path of Hamiltonians that passes through a critical point separating the phases $[1]$ and $[\alpha]$ where $[\alpha]^2 = [1]$. We assume that this critical point is a CFT, and we restrict the path of Hamiltonians to lie in the vicinity of the critical point such that the low-energy spectrum everywhere along the path is reproduced by a Hamiltonian of the form

$$H(\delta) = H_{\text{CFT}} + \delta\Phi \quad (1)$$

where Φ is a perturbation by a relevant operator in the CFT. We expect this scenario, since, generically, the perturbation Φ will open a gap and SPT phases are gapped. Without loss of generality, we assume that $H(\delta)$ is in the trivial phase when $\delta < 0$ and in the nontrivial phase when $\delta > 0$. Next, note that given any Hamiltonian in the trivial SPT phase H_0 , there exists a G -symmetric FDLUC \mathcal{U} for which $H_\alpha \equiv \mathcal{U}H_0\mathcal{U}^\dagger$ is in the nontrivial SPT phase and, additionally, has an identical correlation length. It is argued that \mathcal{U} becomes a symmetry at the critical point. At a minimum, we can conclude that \mathcal{U} is a \mathbb{Z}_2 symmetry, but in some cases it is possible to argue for an even larger emergent symmetry at similar critical points [66,67]. Thus \mathcal{U} (really, the restriction of \mathcal{U} to the low-energy Hilbert space) must precisely be the unitary that changes the sign of the perturbation, i.e., $\mathcal{U}\Phi\mathcal{U}^\dagger = -\Phi$. Further, by the properties of SPT states, we would expect that upon truncating \mathcal{U} to an interval, \mathcal{U} would no longer commute with the global symmetry; instead, the parts of \mathcal{U} deep in the bulk would commute, but the boundary would host a projective representation of G [68]. This should be reflected in the CFT through the 't Hooft

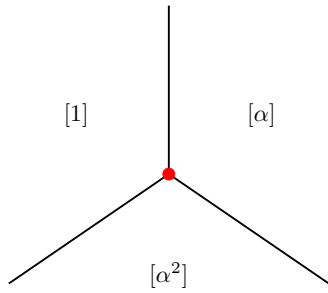


FIG. 3. A hypothetical phase diagram where all N of the $\mathbb{Z}_N \times \mathbb{Z}_N$ SPT phases, where each phase is labeled by its respective class $[i] \in H^2(\mathbb{Z}_N \times \mathbb{Z}_N, U(1)) = \mathbb{Z}_N$, meet at a multicritical point (marked in red), illustrated in particular for the case $N = 3$. The dimension of such a phase diagram increases with N . We expect the multicritical point to possess a mixed anomaly of the kind studied in this paper, and our numerical bounds restrict the properties of CFTs that can describe such multicritical points.

anomaly of the full $\mathbb{Z}_2 \times G$ symmetry, which is captured by a 3-cocycle $\omega \in H^1[\mathbb{Z}_2, H^2(G, U(1))] \subset H^3(\mathbb{Z}_2 \times G, U(1))$. In total, at the critical point \mathcal{U} is an internal symmetry having a mixed anomaly with G , and there exists a relevant operator charged under \mathcal{U} , which drives the transition.

We may now produce a simple generalization of this result to the case of a multicritical point between SPT phases generated by a phase $[\alpha]$ such that $[\alpha]^N = [1]$. Such a family of phases is given, for example, by SPT phases protected by $G = \mathbb{Z}_N \times \mathbb{Z}_N$ for which $H^2(G, U(1)) = \mathbb{Z}_N$, which is relevant to this paper.

In this setting, we may now consider an $(N - 1)$ -parameter family of Hamiltonians

$$H(\delta_1, \dots, \delta_{N-1}) = H_{\text{CFT}} + \sum_i \delta_i \Phi_i \quad (2)$$

and essentially repeat the argument above with minimal modification. The main difference between the previous case and this case is that the FDLUC \mathcal{U} will cyclically permute the N different phases leading to a \mathbb{Z}_N action among the fields that perturb the CFT into the different SPT phases, i.e., $\mathcal{U}\Phi_i\mathcal{U}^\dagger = \sum_j U_{ij}\Phi_j$ with $U^N = I$. We have presented an illustration of such a hypothetical critical point in Fig. 3 for the case $N = 3$.

The transition to the neighboring SPT phases for such a multicritical point would be driven by relevant perturbations that are charged under the emergent \mathbb{Z}_N but preserve the microscopic $\mathbb{Z}_N \times \mathbb{Z}_N$. An interesting class of theories to consider are ones where there are no relevant operators that are symmetric under the full \mathbb{Z}_N^3 symmetry. This is the generic case that is expected without additional fine-tuning. For $N = 3$, we see that such critical points, which do not contain \mathbb{Z}_3^3 -symmetric relevant operators, must have $c \geq 2$ using Fig. 1. On the contrary, with a symmetry-preserving relevant perturbation there could be neighboring phases where \mathcal{U} is an exact lattice symmetry (but, generically, it will not necessarily be a \mathbb{Z}_N symmetry). Due to the anomaly, these phases cannot be trivially gapped and therefore must be SSB or gapless.

III. LSM ANOMALIES ON THE LATTICE AND IN THE CONTINUUM

The microscopic assumptions leading to the generalized LSM theorem manifest in a CFT as a particular set of properties possessed by so-called topological defect lines (TDLs) that implement the symmetries. In this section we first describe the lattice symmetries and anomalies and their relation to those in the continuum field theory. Then, we discuss the continuum description of these symmetries and anomalies using the TDL formalism with emphasis on aspects that enter in bootstrap calculations.

A. Lattice symmetries and anomaly matching

Consider a local lattice system defined on a spatial ring with L sites and a tensor product Hilbert space $\mathcal{H} = \bigotimes_{i=1}^L \mathcal{H}_i$, where the Hilbert space at each site is finite dimensional. We will consider nearest-neighbor Hamiltonians for such a system of the form

$$H = \sum_i H_{i,i+1} \quad (3)$$

where $H_{i,i+1}$ acts on at most the sites $i, i + 1$. The assumption of a nearest-neighbor Hamiltonian is generic under the assumptions of spatial locality and finite on-site Hilbert space dimension, since we may group finitely many sites together for a non-nearest-neighbor Hamiltonian while preserving these assumptions to obtain nearest-neighbor interactions.

As already stated, we will be interested in considering Hamiltonians with symmetry $G_{\text{UV}} = \mathbb{Z}^{\text{trans}} \times \mathbb{Z}_N^2$. We will denote the operator generating unit translations for the system, in the presence of periodic boundary conditions, by T , i.e., for any operator \mathcal{O}_i acting at a single site i we have $T\mathcal{O}_i T^\dagger = \mathcal{O}_{i+1}$. We will also assume that the internal \mathbb{Z}_N^2 is generated by unitary operators of the following form:

$$X = \bigotimes_{i=1}^L X_i, \quad Z = \bigotimes_{i=1}^L Z_i, \\ X^2 = Z^2 = 1, \quad [X, Z] = 0.$$

The key microscopic assumption leading to the LSM anomaly, together with translation symmetry, is that

$$X_i Z_i = e^{2\pi i p/N} Z_i X_i. \quad (4)$$

That is, when the symmetry generators are restricted to a single site they form a projective representation of \mathbb{Z}_N^2 characterized by $\alpha_p \in H^2(\mathbb{Z}_N^2, U(1))$ with

$$\alpha_p(g, h) = \exp\left(\frac{2\pi i}{N} \eta_p(g, h)\right) = \exp\left(\frac{2\pi i p}{N} g_1 h_2\right). \quad (5)$$

Note that the multiplication in the product $g_1 h_2$ should be viewed as multiplication of real numbers, not the group multiplication for \mathbb{Z}_N elements. Of course, all of the aforementioned symmetry generators commute with the Hamiltonian, but in light of (4) the assumed $\mathbb{Z}^{\text{trans}} \times \mathbb{Z}_N^2$ group structure further requires $L = 0 \pmod N$.

To diagnose the anomaly of the system, we may follow, e.g., [9, 69, 70], identifying the anomaly of our $(1 + 1)d$ system as being related to a $(2 + 1)d$ SPT protected by an internal

symmetry. The idea is to consider the degrees of freedom of our original $(1+1)d$ system as being built from a stack of $(1+1)d$ SPTs that terminate at each site of our lattice. The $(1+1)d$ SPT assigned to each lattice site is determined by the projective representation carried by each site, which is uniform in our case and given by (5).

LSM constraints for translation symmetry in $(1+1)d$, related to a $(1+1)d$ SPT class such as α_p as previously discussed, are associated with anomaly 3-cocycles of the form [70]

$$\Omega_{\text{UV}}(g, h, k) = \exp(i\tau(g)\alpha_p(h, k)) \quad (6)$$

where $\alpha_p \in H^2(\mathbb{Z}_N^2, \mathbb{Z}_N)$ and $\tau \in H^1(\mathbb{Z}, \mathbb{Z}) = \mathbb{Z}$. Note that τ may be pulled back to a \mathbb{Z} gauge field whose holonomy around all of space measures the number of lattice sites [69].

At low energy, lattice models of this kind are described by CFTs. CFTs with internal, discrete symmetry G have anomalies valued in $H^3(G, U(1))$ [59]. As stated, in this paper we consider lattice models that flow to CFTs with minimal internal symmetry $G = \mathbb{Z}_N^3$, which comes from the \mathbb{Z} lattice translation symmetry becoming an emanant \mathbb{Z}_N , whose anomaly is given by

$$\omega_{\text{IR}}(g, h, k) = \exp\left(\frac{2\pi i}{N}g_1 h_2 k_3\right). \quad (7)$$

We will refer to ω_{IR} as an ‘‘LSM anomaly’’ in the remainder of this paper, even though as we emphasized previously its interpretation as an LSM anomaly only truly holds at the lattice level in reference to mixed anomalies between spatial and internal lattice symmetries.

The remaining task of this section is to show that the assumed symmetry and anomaly of the CFT is compatible with the anomaly matching constraint of the lattice model. To do this, we must specify a group homomorphism γ from the UV to the IR symmetry groups, and show that the pullback of the IR anomaly cocycle through γ reproduces the UV anomaly cocycle. Denoting an element $g \in G_{\text{UV}}$ by $g = (g_1, g_2, g_3)$ we use the homomorphism $\gamma : \mathbb{Z}^{\text{trans}} \times \mathbb{Z}_N^2 \rightarrow \mathbb{Z}_N^3$,

$$\gamma(g_1, g_2, g_3) = (g_1 \bmod N, g_2, g_3).$$

It is easily seen that $\Omega_{\text{UV}} = \gamma^* \omega_{\text{IR}}$ since Ω_{UV} is only sensitive to $g \in \mathbb{Z}^{\text{trans}} \bmod N$ anyway, and γ is merely the map sending such g to its mod N value. Finally, γ is surjective onto the subgroup $\mathbb{Z}_N^3 \subset G_{\text{IR}}$, so we conclude that the proposed symmetry and anomaly is able to match the symmetry and anomaly of the lattice.

We finally remark that there are other emanant symmetries that could match the anomaly of the lattice. In particular, any cyclic group of the form \mathbb{Z}_{kN} with k a positive integer would suffice, consistent with the mod N periodicity of the translation-twisted boundary conditions. For simplicity, we will not explore these other possibilities further.

B. Topological defect lines

To describe discrete, possibly anomalous, 0-form symmetries in $(1+1)d$ we will follow the TDL formalism as described in Ref. [53], which draws on various earlier works in both physics and mathematics (see [71–76] and other ref-

erences contained therein). In this section, we will review the salient features of the TDL formalism for our paper, but for a more detailed account see Ref. [53].

In modern language, symmetries are implemented by topological operators inserted along subdimensional manifolds of spacetime [53,77]. Invertible 0-form symmetries in $(1+1)d$ are implemented via TDLs, which are associated with oriented, closed curves labeled by elements of a group G . The TDLs are topological, in the sense that their support may be moved freely inside correlation functions so long as the change does not sweep the TDL past a charged operator. An important feature of TDLs is that they commute with the stress tensor. Thus, two operators that are related to each other by action by a TDL must have the same conformal dimensions. The mathematical structure underlying the TDL formalism is that of a fusion category [53,78]. In this paper we will focus on fusion categories $\mathcal{C} = \text{Vec}_G^\omega$ [78], i.e., G -graded vector spaces twisted by a 3-cocycle $\omega \in H^3(G, U(1))$, which describe an anomalous group G symmetry with anomaly ω .

Suppose we have a CFT with an internal symmetry G . To each group element $g \in G$, we associate an extended, oriented topological line operator \mathcal{L}_g , which acts on the primary fields of the theory. Two TDLs \mathcal{L}_g and \mathcal{L}_h supported on topologically equivalent lines may be fused together to create the line \mathcal{L}_{gh} , so the fusion of TDLs obeys the group multiplication law of G . For a given TDL \mathcal{L} , we will denote its orientation reversal (which corresponds to the inverse line when \mathcal{L} is invertible) by $\bar{\mathcal{L}}$. We will denote a unitary operator acting on the Hilbert space \mathcal{H} of local operators, i.e., a TDL \mathcal{L}_g supported on a time slice, by $\hat{\mathcal{L}}_g$, and we will denote the action of such operators on a field ϕ as $\hat{\mathcal{L}}_g \cdot \phi$. TDLs have more explicit constructions as well in terms of topological interfaces between a given CFT and itself, which may be studied via the folding trick [71,79].

A given TDL \mathcal{L}_g may terminate at a point, and at this point will live a *defect operator* [53,72,80]. Such an operator may be constructed through the operator state mapping, since quantizing the theory in a cylinder geometry with a boundary condition twisted by \mathcal{L}_g is equivalent to the theory in radial quantization with a primary field at the origin attached to a TDL. The possible \mathcal{L}_g defect operators, which we will refer to as ϕ^g , live in the *defect Hilbert space* $\mathcal{H}_{\mathcal{L}_g}$ (sometimes we will refer to the defect Hilbert spaces as twisted sectors). More generally, multiple TDLs $\mathcal{L}_{g_1}, \dots, \mathcal{L}_{g_n}$ may terminate at a n -way junction and correspondingly there will be a *junction Hilbert space* $\mathcal{H}_{\mathcal{L}_{g_1}, \dots, \mathcal{L}_{g_n}}$, defined similarly. Due to the fusion properties of the lines, there is an isomorphism between $\mathcal{H}_{\mathcal{L}_{g_1}, \dots, g_n}$ and $\mathcal{H}_{\mathcal{L}_{g_1}, \dots, \mathcal{L}_{g_n}}$. The junction Hilbert space may contain a state, which is proportional to the vacuum of the bulk theory with conformal dimensions $(0,0)$, which is unique for the CFTs we consider in this paper. We denote the space of such states in $\mathcal{H}_{\mathcal{L}_{g_1}, \dots, \mathcal{L}_{g_n}}$ by $V_{\mathcal{L}_{g_1}, \dots, \mathcal{L}_{g_n}}$ and refer to it as the *junction vector space*. Since the TDLs we consider are all invertible, their fusion does not involve direct summation so each $V_{\mathcal{L}_{g_1}, \dots, \mathcal{L}_{g_n}}$ is either one or zero dimensional depending on whether the TDLs forming the junction fuse to the trivial line or not. Thus, there is a single *junction vector* $v \in V_{\mathcal{L}_{g_1}, \dots, \mathcal{L}_{g_n}}$ for each junction, which keeps track of the overall phase associated with each junction, relative to the bulk vacuum state. In Fig. 4 we illustrate a three-way junction, where the ‘‘ \times ’’ keeps

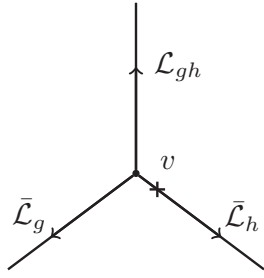


FIG. 4. A three-way junction with junction vector $v \in V_{\mathcal{L}_{gh}, \bar{\mathcal{L}}_g, \bar{\mathcal{L}}_h}$. The convention for the junctions is that we label lines oriented pointing outwards from the junction.

track of the cyclic ordering of the outward-pointing TDLs. The consequences of 't Hooft anomalies may be derived in the TDL formalism using the F -symbol, shown in Fig. 5, which is a map between tensor products of junction vector spaces. The effect of 't Hooft anomalies in this context is to extend the possible symmetry representations of defect operators to include fractionalized and/or projective representations. Specifically, we may construct unitary operators $\hat{\mathcal{L}}_h^g$ that implement the h symmetry in \mathcal{H}_g for any $g, h \in G$. Note that $\hat{\mathcal{L}}_h^g$ depends also on a choice of junction vectors, but we will leave that dependence implicit. The TDL configuration defining this unitary is shown in Fig. 6, which we call the lasso action. To determine aspects of the symmetry action in the defect Hilbert spaces, one may perform a sequence of F-moves to compare $\hat{\mathcal{L}}_h^g \hat{\mathcal{L}}_k^g$ with $\hat{\mathcal{L}}_{hk}^g$, which will be equal up to a phase, i.e.,

$$\hat{\mathcal{L}}_h^g \hat{\mathcal{L}}_k^g = \chi^g(h, k) \hat{\mathcal{L}}_{hk}^g. \quad (8)$$

The phases $\chi^g(h, k)$ are related to the slant products of $[\omega]$, which are topological invariants of the twisted quantum double $\mathcal{Z}(\text{Vec}_G^\omega)$ of Vec_G^ω [81,82]. Using the TDL formalism, the slant product takes the form

$$\chi^g(h, k) = \frac{\omega(g, h, k) \omega(\bar{h}, gh, k) \omega(h, k, \bar{hk})}{\omega(\bar{k}, \bar{h}, ghk) \omega(k, \bar{k}, \bar{h})}. \quad (9)$$

The derivation of (9) is shown in Fig. 7. For each junction vector $v \in V_{\mathcal{L}_g, \mathcal{L}_h, \mathcal{L}_{gh}}$, performing a change of basis $v \rightarrow \beta(g, h)v$ for a $U(1)$ rotation by the 2-cochain $\beta(g, h)$ leads to a change

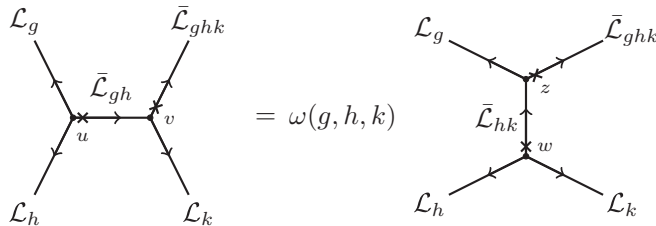


FIG. 5. For any configuration of invertible TDLs involving external TDLs g, h, k and $(ghk)^{-1}$, there are two ways to resolve the configuration into one involving only three-way junctions. The two decompositions differ by a 3-cocycle phase ω . We leave implicit the dependence of ω on the junction vectors appearing in the diagram.

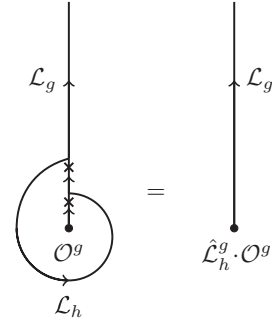


FIG. 6. In each defect Hilbert space \mathcal{H}_g the unitary $\hat{\mathcal{L}}_h^g$ implementing the action of an element $h \in G$ can be defined by wrapping an h -TDL counterclockwise around a defect operator \mathcal{O}^g inserted at the origin (in radial quantization) and collapsing the loop down to a point, as shown. This defines the action $\hat{\mathcal{L}}_h^g|\mathcal{O}^g\rangle$ on states in \mathcal{H}_g . We will take $U \cdot \mathcal{O} \equiv U\mathcal{O}U^\dagger$ to mean conjugation of \mathcal{O} by the unitary U . One can also perform an F move on this configuration to obtain a different convention for resolving the symmetry action, which would differ possibly from this one by a phase for invertible TDLs. Note that if g is the trivial line this reduces to the usual way that symmetry acts on local operators.

in ω [53]

$$\omega(g, h, k) \rightarrow \omega(g, h, k) \frac{\beta(h, k)\beta(g, hk)}{\beta(g, h)\beta(gh, k)}. \quad (10)$$

One may easily verify that the following quantity [36]

$$\iota_g(h, k) = \frac{\chi^g(h, k)}{\chi^g(k, h)}$$

is an invariant of $[\omega]$ under an arbitrary change of basis in the junction vector spaces. When $\iota_g(h, k)$ is nontrivial the symmetry generators do not commute in the defect Hilbert space, signifying a nontrivial projective representation since the symmetry generators commute when acting on the Hilbert space of local operators. The symmetry properties of defect operators under the full internal symmetry group of the theory can be thought of as topological invariants, which lead to a finer classification of CFTs enriched by symmetries. For recent explorations of this idea, see e.g., Ref. [83].

One class of 't Hooft anomalies that have been studied in recent modular bootstrap work involve a single \mathbb{Z}_N . These so-called type-I anomalies manifest as anomalous spin-selection rules in the defect Hilbert spaces, which can be directly used as input into the modular bootstrap [30,31]. In contrast, we will be mostly interested in type-III anomalies [84,85], of which the continuum LSM anomaly is a particular case, whose signatures are more subtle, involving defect operators in the defect Hilbert spaces of one \mathbb{Z}_N subgroup transforming in a nontrivial projective representation of the remaining \mathbb{Z}_N^2 subgroup.

We will now summarize the consequences of each of these two classes of anomalies on the operator content of CFTs, each of which generally appears in the theories we consider.

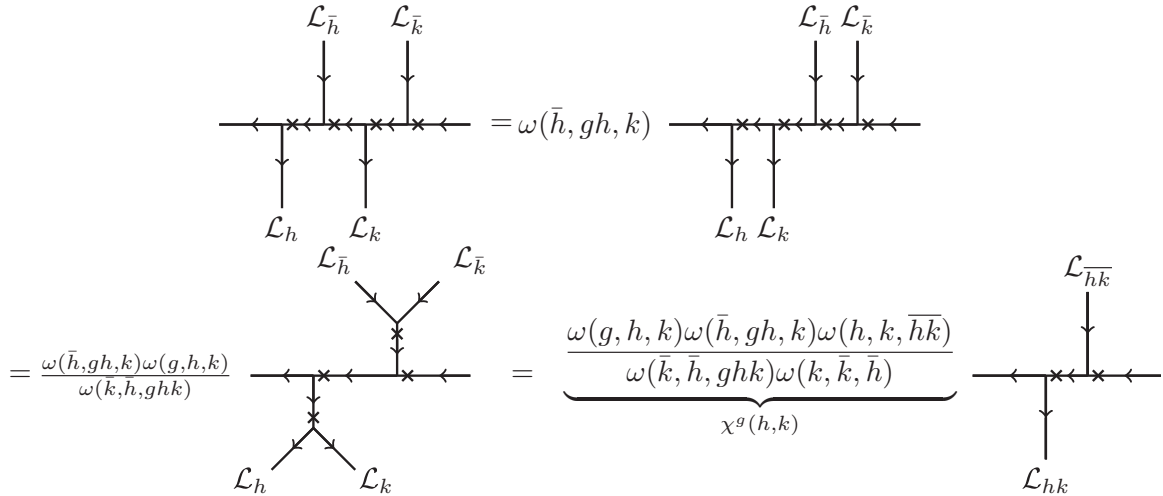


FIG. 7. The graphical derivation of the slant product formula for $\chi^g(h, k)$. This diagram should be considered as part of a larger diagram in which the \mathcal{L}_h and \mathcal{L}_k TDLs are connected and each encircle a defect operator \mathcal{O}^g , as in the lasso diagram of Fig. 6. The final step in the derivation involves the phase factor associated with shrinking the bubble of the composite line \mathcal{L}_{gh} . This factor is determined by using the single bubble to create a second identical bubble using a sequence of F moves, which allows the phase associated with a single bubble to be determined.

1. Type-I anomalies

In the case that G has a \mathbb{Z}_M subgroup, the subgroup may have a \mathbb{Z}_M or “type-I” anomaly [84]. In particular, the restriction of the full cocycle, which encodes the full anomaly of G , to this subgroup may be cohomologous to [84]

$$\omega(a, b, c) = \exp\left(2\pi i \frac{ka}{M^2}(b + c - [b + c]_M)\right) \quad (11)$$

where $a, b, c \in \mathbb{Z}_M$ and $[k] \in \mathbb{Z}_M = H^3(\mathbb{Z}_M, U(1))$ labels the anomaly. Note that $[a + b]_M \equiv a + b \pmod{M}$. The main signature of a TDL \mathcal{L}_g generating a \mathbb{Z}_M symmetry with anomaly $[k]$ is that the defect Hilbert space \mathcal{H}_g will contain states whose spins are in [53]

$$s \in k/M^2 + \mathbb{Z}/M. \quad (12)$$

Nonzero k thus corresponds to an anomalous spin selection rule for the defect operators. We will refer to a TDL generating a \mathbb{Z}_M subgroup as nonanomalous if $k = 0$ and anomalous otherwise. The anomaly forces the minimum possible scaling dimension for a defect operator on such a TDL to be $\Delta = \min(\frac{|k|}{M^2}, \frac{|k-M|}{M^2})$ as opposed to $\Delta = 0$ for a nonanomalous TDL.

A \mathbb{Z}_M anomaly can be detected by, for instance, studying the torus partition function of the theory twisted by symmetry defects and imposing covariance of the partition function under the modular S transformation, see e.g., Refs. [30,31]. To deduce the spin selection rule of a TDL \mathcal{L}_g , with g generating a \mathbb{Z}_M subgroup, given any 3-cocycle ω , we can use the formula

$$e^{2\pi i Ms} = \prod_{i=1}^{M-1} \omega(g^{-1}, g^i, g) \quad (13)$$

given in Ref. [86] and solve for the allowed values of s . The \mathbb{Z}_M anomalies possessed by theories with the LSM anomalies that we study are listed in Table I.

2. Type-III anomalies

The LSM anomalies (7) we consider, reproduced below for convenience with $p = 1$ and henceforth referred to as ω ,

$$\omega(g, h, k) = \exp\left(\frac{2\pi i}{N} g_1 h_2 k_3\right) \quad (14)$$

are examples of “type-III” anomalies. The signature of this anomaly in CFT is that defect operators of one \mathbb{Z}_N subgroup transform in a projective representation of the remaining $\mathbb{Z}_N \times \mathbb{Z}_N$ subgroup.

More specifically, let g_1, g_2 , and g_3 be the generators of the three \mathbb{Z}_N subgroups in \mathbb{Z}_N^3 . Let us now consider a defect operator that lives at the end of a TDL \mathcal{L}_{g_1} . One can show using $\chi^{g_1}(g_2, g_3)$ that, in the presence of \mathcal{L}_{g_1} , the TDLs \mathcal{L}_{g_2} and \mathcal{L}_{g_3} no longer commute when the \mathbb{Z}_N^3 symmetry has the anomaly (14). For illustrative purposes, the unitaries $\hat{\mathcal{L}}_{g_2}^{g_1}$ and $\hat{\mathcal{L}}_{g_3}^{g_1}$ may be taken to satisfy

$$\hat{\mathcal{L}}_{g_2}^{g_1} \hat{\mathcal{L}}_{g_3}^{g_1} = e^{2\pi i/N} \hat{\mathcal{L}}_{g_3}^{g_1} \hat{\mathcal{L}}_{g_2}^{g_1} \quad (15)$$

[i.e., $\chi^{g_1}(g_2, g_3) = e^{2\pi i/N}$] meaning g_2, g_3 are realized projectively. Thus, the entire g_1 defect Hilbert space decomposes as a direct sum of such projective representations since the choice of defect operator is arbitrary.

A convenient basis for such $\mathbb{Z}_N \times \mathbb{Z}_N$ projective representations is the clock and shift basis. In this basis, g_2 is diagonalized so that states in \mathcal{H}_{g_1} carry definite g_2 charge. Then, g_3 acts as a shift operator, which increases g_2 charge by one modulo N . That is, we can choose primary fields $\phi_0^{g_1}, \dots, \phi_{N-1}^{g_1}$ in \mathcal{H}_{g_1} , all with identical conformal dimensions, such that

$$\hat{\mathcal{L}}_{g_2}^{g_1} \cdot \phi_I^{g_1} = e^{2\pi i I/N} \phi_I^{g_1}, \quad (16)$$

$$\hat{\mathcal{L}}_{g_3}^{g_1} \cdot \phi_I^{g_1} = \phi_{[I+1]_N}^{g_1}. \quad (17)$$

From this, we see that given a single primary field in \mathcal{H}_{g_1} we can infer the existence of $N - 1$ more fields of the same conformal dimensions. Additionally, since a unitary CFT has a well-defined Hermitian conjugate, when $g_1 \neq g_1^{-1}$ there also must exist N more fields living in $\mathcal{H}_{g_1^{-1}}$. Thus, we see that a feature of theories with the \mathbb{Z}_N^3 LSM anomaly is that the degeneracy of Virasoro defect primary fields with fixed conformal dimensions is a multiple of N when the defect corresponds to an order N element of G .

C. Gauging nonanomalous TDLs

A CFT with $G = \mathbb{Z}_N^3$ and the LSM anomaly described above contains various nonanomalous TDLs, which, consequently, may be gauged (in CFT terminology, orbifolded). For the parts of our calculations involving correlation functions of defect operators, it will be somewhat simpler to view things from the point of view of the gauged theory since, from this perspective, many of the technicalities one needs to be aware of when working with defect operators can be avoided [87].

Let $H = \mathbb{Z}_N$ be such a nonanomalous \mathbb{Z}_N subgroup. Given some CFT \mathcal{T}_{LSM} with the LSM anomaly, when we gauge H we end up with a new theory $\tilde{\mathcal{T}}_{\text{LSM}} = \mathcal{T}_{\text{LSM}}/H$, which generally will have a different spectrum of local operators. The gauging procedure amounts to first throwing away all local operators that are charged under H , leaving only the H -invariant operators. This theory, keeping just symmetric local operators, will generically not be modular invariant, so in addition to the H -invariant local operators we must also bring down H -invariant defect operators from the H -twisted sectors [80,88–90]. Due to the spin-charge relation for defect operators [30,31], this amounts to adding all integer spin defect operators from the H -twisted sectors. Since $H^2(\mathbb{Z}_N, U(1))$ is trivial, we do not additionally need to specify a discrete torsion class as another ingredient to this gauging procedure [80,88].

When a set of TDLs is gauged, the gauged theory will, in general, possess a different set of TDLs from the ungauged theory. We may conclude various facts about the TDLs of $\tilde{\mathcal{T}}_{\text{LSM}}$ with the help of some results contained, for instance, in Ref. [90] and also Ref. [91]. The key thing to note is that local operators must transform in *linear* representations, but, at first sight, the defect operators coming from \mathcal{T}_{LSM} , which are promoted to local operators of $\tilde{\mathcal{T}}_{\text{LSM}}$, transform in projective representations of the $G/H = \mathbb{Z}_N^2$ symmetry. Thus, to restore a linear representation of this symmetry in $\tilde{\mathcal{T}}_{\text{LSM}}$, the projective phases $\chi^g(h, k)$ for $g \in H, h, k \in G/H$ are promoted into central elements of the symmetry group \tilde{G} of $\tilde{\mathcal{T}}_{\text{LSM}}$, so we can identify \tilde{G} as a central extension of G/H by H with presentation

$$\langle a, b, c | a^N, b^N, c^N, aba^{-1}b^{-1}c^{-1}, aca^{-1}c^{-1}, bcb^{-1}c^{-1} \rangle. \tag{18}$$

In $\tilde{\mathcal{T}}_{\text{LSM}}$, the operators transforming in one-dimensional irreducible representations (irreps) of \tilde{G} were local operators in \mathcal{T}_{LSM} , and operators transforming in higher dimensional irreps were defect operators of \mathcal{T}_{LSM} .

When N is prime, the groups with presentation given by (18) are known as Heisenberg groups $\text{He}(3, \mathbb{Z}_N)$. When $N = 2$, we can also identify $\text{He}(3, \mathbb{Z}_2) \cong D_8$ where D_8 is the square dihedral group. This particular case of gauging

was studied in a rather different context in Ref. [92]. When N is not prime, the representation theory of the groups that we might still call $\text{He}(3, \mathbb{Z}_N)$ differs from the prime case. In mathematics literature such groups have a different naming convention, but we will still refer to groups with presentation (18) as $\text{He}(3, N)$.

We imported information about the representation theory of the groups $\text{He}(3, N)$ with the help of GAP [93]. For each N we consider, the information about the corresponding group is contained in the `SmallGroups` library. The `SmallGroups` identification numbers for the groups are (8,3), (27,3), (64,18), (125,3), and (216,77) for $N = 2, \dots, 6$. We will label representations of $\text{He}(3, N)$ by R_n where n is the index of the representation in GAP.

D. Comments on correlation functions of defect operators

The OPE is a mapping between two separated local fields ϕ_a, ϕ_b and linear combinations of local fields at a single point, schematically expressed as

$$\phi_a \times \phi_b \sim \sum_{\mathcal{O}} \lambda_{\phi_a \phi_b \mathcal{O}} \mathcal{O}$$

where the (possibly complex) numbers $\lambda_{\phi_a \phi_b \mathcal{O}}$ are called the OPE coefficients, and $\bar{\mathcal{O}}$ denotes the Hermitian conjugate of \mathcal{O} .

The OPE can also be taken between defect operators, but it has a slightly different interpretation, since in general the inputs and outputs of the defect OPE will live in different defect Hilbert spaces. Again schematically, if we take defect operators living at the ends of TDLs \mathcal{L}_g and \mathcal{L}_h , their OPE can be written as follows:

$$\phi_a^g \times \phi_b^h \sim \sum_{\mathcal{O}^{gh}} \lambda_{\phi_a^g \phi_b^h \mathcal{O}^{gh}}^v \mathcal{O}^{gh}$$

where we use the notation $\bar{g} \equiv g^{-1}$. It is important to note that OPE coefficients of defect operators depend, up to a phase, on a junction vector v . This is because in order to calculate the OPE coefficient, one constructs a four-point function containing three defect operators together with a junction vector connecting the TDLs of the defect operators in a configuration such as that of Fig. 4, with defect operators added to ends of the TDLs. Further, since there are three different junction vectors for a given three-way junction (when the TDLs forming the junction are all invertible), there is freedom to choose a junction vector when writing down OPE coefficients. Thus, there is a separate OPE coefficient for each junction vector, but all choices are related to each other in a fixed way via the cyclic permutation map between junction vector spaces [53], which results in an overall phase difference. Strictly speaking, the OPE coefficient for defect operators may also depend on the angle of the TDL leaving the defect operators, but since we deal only with scalar defect operators, which transform trivially under rotations, we do not encounter this complication.

In the most general setting, there are a few differences that must be accounted for when considering correlation functions of defect operators. First of all, the nonlocal nature of the defect operators leads, in some cases, certain correlation functions of defect operators to be multivalued maps of the positions of the operators in the correlation function. This

is because winding an operator charged under the TDL attached to a defect operator must involve acting on the charged operator with the TDL. Additionally, defect operators obey a modified version of crossing symmetry. A correlation function of four defect operators is really a six-point function of the defect operators along with two junction vectors, which can be represented graphically by attaching defect operators to the TDLs in the left-hand side of the graphical equation in Fig. 5. Crossing symmetry is then modified since there may be a phase $\omega(g, h, k)$ accrued when relating the two OPE channels of the four external operators. Further, the intermediate operators will live in potentially different defect Hilbert spaces. For more discussion on correlation functions of defect operators, see Refs. [94,95].

Appealing to the gauging argument from the previous subsection, we will now argue that the version of crossing symmetry obeyed by the scalar defect operators we consider in this paper is identical to certain local operators. Again, let \mathcal{T}_{LSM} be defined as before and $H = \mathbb{Z}_N$ be a nonanomalous subgroup of $G = \mathbb{Z}_N^3$. Consider external defect operators $\phi_I^g, \bar{\phi}_I^g$, for $I = 1, \dots, N$, where we take g to generate H . Since scalar defect operators are neutral under H , upon gauging H they are promoted to local operators in $\tilde{\mathcal{T}}_{\text{LSM}}$ that, without loss of generality, can be taken to transform in representations $R_{N^2+1}, \bar{R}_{N^2+1}$ of $\text{He}(3, N)$, which are N -dimensional irreps. Since all operators appearing in OPEs of the defect operators $\phi_I^g, \bar{\phi}_I^g$ will also be neutral under H by \mathbb{Z}_N charge conservation, gauging does not modify the values of the correlation functions that they generate. In particular, this means that it must be possible to set the extra phase that could appear in Fig. 5 equal to 1 since we can exactly relate the value of the defect operator correlation function to a correlation function involving only local operators via gauging. Thus, for the purpose of bootstrap, the crossing equations we generate from viewing the external operators as defect operators in \mathcal{T}_{LSM} or local operators in $\tilde{\mathcal{T}}_{\text{LSM}}$ will be identical. We should note, however, that if one wants to strictly think of everything in terms of defect operators, an analogous statement is that all the phases $\omega(\bar{g}, \bar{h}, \bar{k})$ can be set equal to 1 for the four-point functions we consider, which only involve TDLs corresponding to elements of H , by a careful choice of junction vectors, which is done partially in Appendix A of Ref. [53]. We note that, for these reasons, we may drop all dependence on junction vectors from the diagrams we draw and formulas we write down. This is reflected in the diagrams representing the four-point functions we consider, as in Fig. 8.

IV. NUMERICAL BOOTSTRAP APPROACH

The bounds presented in the main results section are obtained via an approach that uses correlator bootstrap bounds as additional input to modular bootstrap, thereby augmenting the usual procedure to incorporate global symmetries into modular bootstrap. Here we outline the details of how our bounds are obtained.

A. Correlator bootstrap with defect operators

We first will show both how the local operator spectrum and central charge of unitary CFTs with a $G = \mathbb{Z}_N^3$ internal

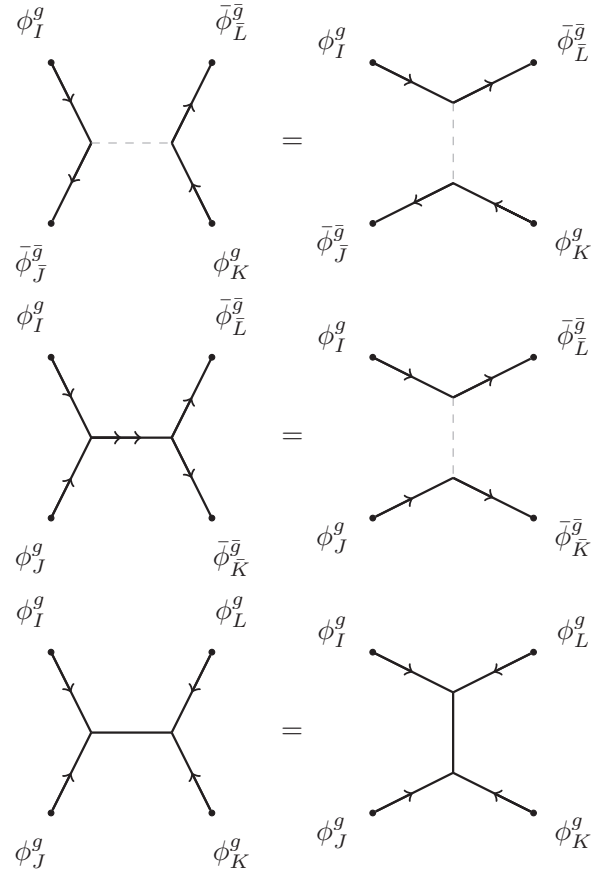


FIG. 8. A pictorial representation of the four-point functions of defect operators that we impose crossing symmetry on in our bootstrap calculations. In these configurations, all the external TDLs are either \mathcal{L}_g or $\bar{\mathcal{L}}_g$. The internal TDL marked by a double arrow represents \mathcal{L}_{g^2} , but when \mathcal{L}_{g^2} squares to the trivial line, like when $N = 4$, we denote it by an orientationless TDL such as in the bottom diagram. When $N = 2$ all diagrams are equivalent. For general $N > 2$, only the top and middle diagrams are consistent with the group multiplication except when $N = 4$ where the bottom diagram is consistent as well. Due to the gauging argument, we can neglect the dependence on the junction vectors since there is a canonical choice that removes the phase $\omega(g, h, k)$ in our cases, which involve only external defect operators hosted on a single \mathbb{Z}_N TDL or its inverse. We could also even consider these to be correlation functions of local operators, but to emphasize the more generic scenario we stick to drawing defect operators.

symmetry and LSM anomaly are constrained when there is an additional assumption that the theory possesses certain light defect operators hosted on TDLs of the theory. To obtain central charge bounds, we additionally assume a nongeneric gap, the value of which we scan over, to the scaling dimension of any local operator appearing in the OPEs of the defect operators.

To do correlator bootstrap, one must first derive the crossing symmetry constraints arising from all possible four-point functions involving the external operators under consideration. Deriving these constraints by hand is rather cumbersome. Since we know the bootstrap equations for the defect operators of interest are equivalent to those of local operators

transforming in N -dimensional irreps of $\text{He}(3, N)$, we use the autoboot package by Go and Tachikawa to generate the semidefinite constraints [96]. autoboot is a tool specially designed for producing the crossing symmetry constraints for fields transforming in arbitrary global symmetry representations [97]. Here we simply summarize the constraints we impose in an abstract form and list the spectrum assumptions used for semidefinite programming; the constraints themselves are generally too unwieldy to report here, but can be made available upon request or simply obtained via autoboot.

The output of autoboot is a set of vector-matrix-valued functions of the conformal cross-ratios $\mathbf{V}_{R, \Delta, s}^{\Delta_D}(x, \bar{x})$ (i.e., vectors whose components are matrices, with the matrix entries being functions of the conformal cross ratios), each of which represents the crossing symmetry constraint due to external fields with scaling dimension Δ_D transforming in N -dimensional irreps of $\text{He}(3, N)$ and internal fields transforming in a representation R with scaling dimension Δ and spin s . We take the functions $\mathbf{V}_{R, \Delta, s}^{\Delta_D}(x, \bar{x})$ to have components expressed in terms of the global conformal blocks for $(1+1)d$ CFTs, given by [98,99]

$$g_{\Delta, s}(x, \bar{x}) = \frac{(-2)^{-s}}{1 + \delta_{s,0}} (k_{\Delta+s}(x)k_{\Delta-s}(\bar{x}) + k_{\Delta-s}(x)k_{\Delta+s}(\bar{x})) \quad (19)$$

where

$$k_\beta(x) = x^{\beta/2} {}_2F_1\left(\frac{\beta}{2}, \frac{\beta}{2}, \beta, x\right). \quad (20)$$

Each component of the vectors $\mathbf{V}_{R, \Delta, s}^{\Delta_D}(x, \bar{x})$ corresponds roughly to a distinct four-point function, although the actual implementation in autoboot combines different four-point functions using certain invariant tensors of the symmetry group. If we denote all distinct OPE coefficients, where the internal field is \mathcal{O}_R and where we use I, J to label different choices of external fields, by $\lambda_{I\mathcal{O}_R}$ (i.e., I labels a pair of fields here), we can compactly express the crossing symmetry constraints as

$$\sum_{I, J} \sum_R \sum_{\mathcal{O}_R} \lambda_{I\mathcal{O}_R} \lambda_{J\mathcal{O}_R} [\mathbf{V}_{R, \Delta_{\mathcal{O}_R}, s_{\mathcal{O}_R}}^{\Delta_D}]^{kJI} = 0 \quad (21)$$

for each k , indexing the different individual crossing symmetry constraints. Note that the OPE coefficients in (21) can be chosen to be real [96].

We now proceed with the usual bootstrap algorithm: We make some assumptions about the spectrum of operators of a given theory and see if our assumptions leads to a violation of (21) using semidefinite programming.

To do the semidefinite programming, we will use SDPB [46] to search for a (matrix-valued) linear functional acting on the space of vector-matrix-valued functions of x, \bar{x} that obeys a number of semi-definiteness properties. For our purposes α may be expressed in a basis of derivatives of the cross ratios evaluated at the crossing-symmetric point $x, \bar{x} = \frac{1}{2}$,

$$\alpha[\mathbf{V}(x, \bar{x})] = \sum_k \sum_{\substack{m, n=0 \\ m+n \leq \Lambda^{\text{cor}}}}^{\Lambda^{\text{cor}}} a_{mn}^k \partial_x^m \partial_{\bar{x}}^n [\mathbf{V}(x, \bar{x})]^k \Big|_{x=\bar{x}=\frac{1}{2}} \quad (22)$$

where Λ^{cor} is the correlator bootstrap derivative order. The properties we need α to obey will depend on whether we are obtaining upper bounds on scaling dimensions or lower bounds on central charge. In the remaining part of this section we explain the constraints on the linear functional in each of these contexts.

1. Upper bounds on scaling dimension

In order to obtain upper bounds on the scaling dimension of local operators, we will assume that there exist some scalar defect operators $\phi_I^g, \bar{\phi}_I^g$, which have the lowest scaling dimension, equal to Δ_D , among all defect operators in the defect Hilbert spaces corresponding to nonanomalous, order N TDLs. Recall that we label irreps of $\text{He}(3, N)$ as R_i according to their index in GAP. For the purposes of bootstrap, we may take these defect operators as transforming in the representation $R_{N^2+1}, \bar{R}_{N^2+1}$ of $\text{He}(3, N)$ when N is prime or, when $N = 4, 6$, transforming in R_{21}, R_{54} respectively—all such irreps are N dimensional. For brevity later, we will denote the set of all N -dimensional irreps by $[N]$. Taking OPEs of these defect operators may produce either local operators or defect operators. This can be seen in the gauged language by observing first that

$$R_{N^2+1} \otimes \bar{R}_{N^2+1} = \bigoplus_{i=1}^{N^2} R_i$$

where on the right-hand side all direct summands are one-dimensional irreps. Note that this is the only possibility for $N = 2$ since in this case R_5 is a real representation. The one-dimensional irreps can be viewed as representations of \mathbb{Z}_N^3 , and thus we see that the anomaly forces the OPE of the defect operators to contain \mathbb{Z}_N^3 -charged operators. For $N > 2$ we also have

$$N \text{ prime: } R_{N^2+1} \otimes R_{N^2+1} = NR_{N^2+2}$$

$$N = 4: R_{21} \otimes R_{21} = \bigoplus_{i=17}^{20} 2R_i$$

$$N = 6: R_{54} \otimes R_{54} = 3R_{47} \oplus 3R_{49} \oplus 3R_{51} \oplus 3R_{53}.$$

When N is prime, the above tensor products decompose into a direct sum of N copies of another N dimensional irrep, and when $N = 4, 6$ the decomposition is achieved by a combination of irreps of dimension $N/2$. These tensor product decompositions reflect, in the TDL language, that, for prime N , taking the OPE of identical defect operators living on a nonanomalous, order N TDL produces defect operators, which also live on order N , nonanomalous TDLs. Thus, the scaling dimensions of such operators, when they are scalar, are bounded from below by Δ_D . For our cases $N = 4, 6$ this is not the case; instead, two such defect operators create defect operators living on an order $N/2$ nonanomalous TDL, and we make no assumption about the spectrum of such operators beyond what is guaranteed by unitarity.

We now describe how to rule out various assumptions on the scaling dimension of the lightest operators appearing in the OPE of defect operators with the above listed properties. For all N we refer to an operator transforming in *any* nontrivial one-dimensional representation of $\text{He}(3, N)$, which

can be interpreted as an operator transforming in a nontrivial representation of \mathbb{Z}_N^3 , as a charged operator, and refer to an operator transforming in the trivial representation as a symmetric operator. We will denote the assumed minimum scaling dimensions of any scalar symmetric/charged local operator appearing in the OPE of the defect operators by $\Delta_0^{\min}, \Delta_Q^{\min}$ respectively. We will use $[0]$ and $[Q]$ to denote, respectively, the set of trivial and nontrivial one-dimensional irreps. We will refer to these minimum scaling dimensions $\Delta_0^{\min}, \Delta_Q^{\min}$ as the gaps. To attempt to rule out these gaps, we seek a linear functional α of the form (22), satisfying

$$\alpha[\mathbf{V}_{R_i,0,0}^{\Delta_D}] = 1$$

$$\alpha[\mathbf{V}_{R_i,\Delta,s}^{\Delta_D}] \geq 0 \quad \forall \Delta \geq \begin{cases} \Delta_0^{\min} & R_i \in [0], s = 0 \\ \Delta_Q^{\min} & R_i \in [Q], s = 0 \\ \Delta_D & R_i \in [N], s = 0, \quad N \text{ odd} \\ |s| & \text{else} \end{cases}$$

where $M \geq 0$ for a real, symmetric matrix M means that M is positive semidefinite. It is necessary to truncate the values of spin for which we impose the above constraints to only include $|s| \leq S_{\max}^{\text{cor}}$, which we choose to be sufficiently large so that our bounds at fixed Λ^{cor} are stable to an increase in S_{\max}^{cor} . Upon finding such a linear functional, we would conclude that the given assumptions are inconsistent with crossing symmetry of the defect operators. If $\Delta_0^{\min} = 0$, we would conclude that Δ_Q^{\min} is an upper bound on the lightest charged operator appearing in the OPE of the defect operators. If $\Delta_0^{\min} = \Delta_Q^{\min} = \Delta^{\min}$, we conclude that Δ^{\min} is an upper bound on the lightest operator of any charge.

Finally, we will denote by $\Delta_Q^*(N, \Delta_D)$ the optimal, to within some small numerical tolerance, upper bound on the scaling dimension of the lightest charged, local, scalar, operator, which appears in the OPE of scalar defect operators transforming in the $R_{N^2+1}, \bar{R}_{N^2+1}$ representations of $\text{He}(3, N)$ with scaling dimension Δ_D . These bounds are shown in Fig. 9. We note that we found the bounds to remain unchanged upon doing similar calculations with $\Delta_0^{\min} = \Delta_Q^{\min}$, i.e., the resulting bound is on the lightest local operator. We do not present bounds on the lightest symmetric operator since our bounds could not guarantee that the OPE of defect operators must produce a relevant symmetric scalar for any choice of Δ_D , so we do not consider such bounds to be particularly interesting.

2. Lower bounds on central charge

For the central charge bounds, we will assume N is odd and prime since these are the cases for which we are most interested in refining our bounds.

Every unitary, $(1+1)d$ CFT possesses conserved, spin-2, quasiprimary fields, which are the holomorphic and antiholomorphic stress tensor fields $T(z), \bar{T}(\bar{z})$. With the appropriate normalization [43], the OPE coefficient of a primary field ϕ with scaling dimension Δ , its conjugate, and the stress tensor is given in $(1+1)d$ by [100]

$$\lambda_{\phi\bar{\phi}T} = \frac{2\sqrt{\dim R}\Delta}{\sqrt{c}},$$

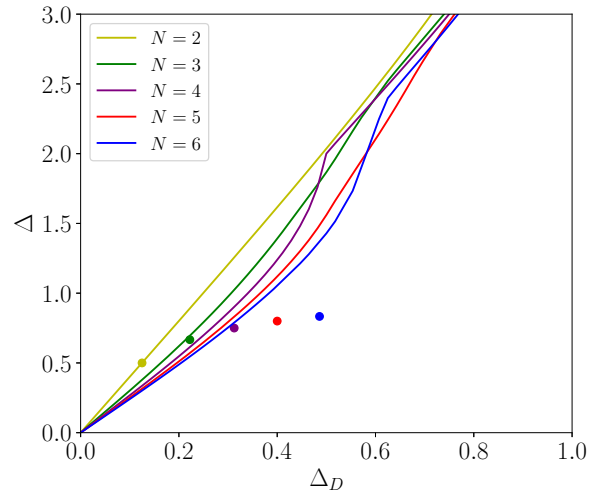


FIG. 9. Upper bounds on the scaling dimension of the lightest \mathbb{Z}_N^3 charged, scalar operator appearing in the OPE of scalar defect operators with scaling dimension Δ_D living on a nonanomalous \mathbb{Z}_N TDL in theories with the LSM anomaly for $N = 2, \dots, 6$. The bound is not noticeably changed if the bound is calculated instead for the lightest local operator transforming in any representation of \mathbb{Z}_N^3 . For each N we assign different colors. The matching colored dots indicate, for each N , points corresponding to the scaling dimension of the lightest \mathbb{Z}_N^3 -charged local operator appearing in the OPE of the lightest scalar \mathbb{Z}_N defect operator living on a nonanomalous \mathbb{Z}_N TDL for $\mathfrak{su}(N)_1$. The $\mathfrak{su}(N)_1$ points for $N = 2, \dots, 6$ are $(\frac{1}{8}, \frac{1}{2}), (\frac{2}{9}, \frac{2}{3}), (\frac{5}{16}, \frac{3}{4}), (\frac{2}{5}, \frac{4}{5}),$ and $(\frac{35}{72}, \frac{5}{6})$. These bounds were computed with $\Lambda^{\text{cor}} = 25$ and $S_{\max}^{\text{cor}} = 50$.

where R is the representation of the internal symmetry group that ϕ transforms in. In the following we will take $\dim R = N$, applicable to the cases that we consider.

To bound the central charge, we again consider some defect operators $\phi_T^s, \bar{\phi}_T^s$ whose scaling dimension is Δ_D . We then expand (21) as

$$0 = [\mathbf{V}_{R_i,0,0}^{\Delta_D}]^k + \lambda_{\phi^s\bar{\phi}^sT}^2 [\mathbf{V}_{R_i,2,2}^{\Delta_D}]^k + \sum_{I,J} \sum_R \sum_{\substack{\mathcal{O}_R \neq T,T \\ \Delta_{\mathcal{O}_R} > 0}} \lambda_{I\mathcal{O}_R} \lambda_{J\mathcal{O}_R} [\mathbf{V}_{R_i,\Delta_{\mathcal{O}_R},s_{\mathcal{O}_R}}^{\Delta_D}]^{kJ}. \quad (23)$$

We now act on (23) with a linear functional of the form (22)

$$\alpha[\mathbf{V}_{R_i,2,2}^{\Delta_D}] = 1$$

$$\alpha[\mathbf{V}_{R_i,\Delta,s}^{\Delta_D}] \geq 0 \quad \forall \Delta \geq \begin{cases} \Delta^{\min} & \text{if } R_i \in [0] \cup [Q], s = 0 \\ \Delta_D & \text{if } R_i \in [N], s = 0 \\ |s| & \text{otherwise} \end{cases}.$$

Note that here we have assumed that the scaling dimension of any scalar, local operator appearing in the OPE of the external defect operators has scaling dimension at least Δ^{\min} . It is necessary to impose some gap in the spectrum of symmetric, scalar operators in order to obtain any central charge bounds, since otherwise we would not be able to have $\alpha[\mathbf{V}_{R_i,0,0}^{\Delta_D}] < 0$. Acting with such a functional and rearranging terms allows us to conclude

$$\lambda_{\phi^s\bar{\phi}^sT}^2 = \frac{4N\Delta_D^2}{c} \leq -\alpha[\mathbf{V}_{R_i,0,0}^{\Delta_D}],$$

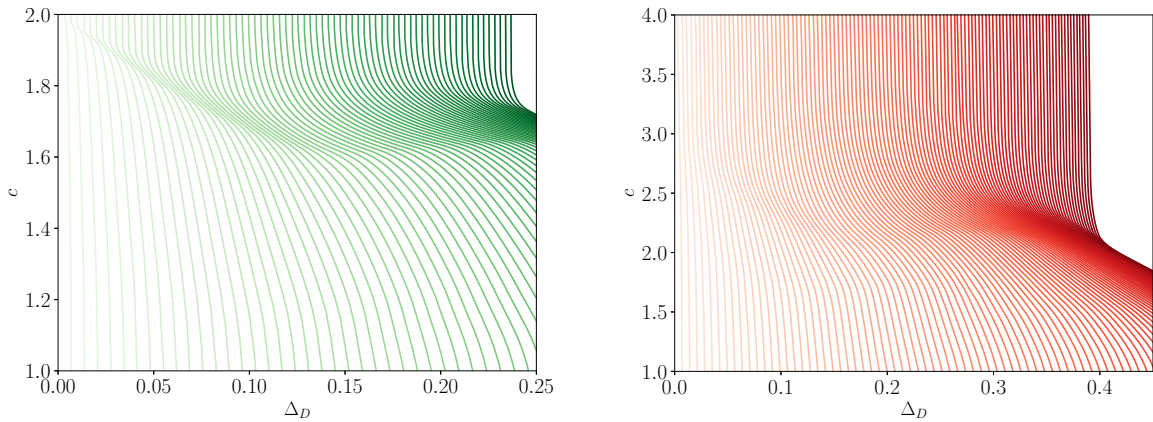


FIG. 10. Lower bounds on central charge for $N = 3$ (left) and $N = 5$ (right) as a function of the scaling dimension of the lightest scalar defect operator living on an order N nonanomalous TDL in a theory with the LSM anomaly. Each solid curve represents a different value of the minimum scaling dimension for the lightest scalar, local operator appearing in the OPE of the external defect operators. For $N = 3$ we compute the curves for values where the gap to the minimum value of the scaling dimension for such operators is $\Delta = 0.01, \dots, 0.75$ and, for $N = 5$, $\Delta = 0.01, \dots, 1.05$, each with spacing 0.01 between successive values. The darkness of the curve indicates the value of the gap from low to high with increasing darkness. For $N = 3$, the computed values of the central charge lower bound are less than $c = 2$, and for $N = 5$ all computed values are less than $c = 4$, in agreement with known theories. To obtain these bounds we used $\Lambda^{\text{cor}} = 15$ with $S_{\text{max}}^{\text{cor}} = 30$.

which means, assuming $-\alpha[\mathbf{V}_{R_1,0,0}^{\Delta_D}] > 0$ consistent with a gap Δ^{min} not being ruled out,

$$c \geq \frac{4N\Delta_D^2}{-\alpha[\mathbf{V}_{R_1,0,0}^{\Delta_D}]} \quad (24)$$

Thus, we want to minimize $-\alpha[\mathbf{V}_{R_1,0,0}^{\Delta_D}]$ consistent with the previously stated constraints to find the strongest lower bound on c , which is again done using SDPB. We will denote our lower bounds obtained in this way, which are presented in Fig. 10, by $c^*(N, \Delta_D, \Delta^{\text{min}})$. Central charge bounds in $(1+1)d$ CFT have been obtained in other papers, e.g., in Ref. [101], so in order to verify the correctness of our setup, we reproduced some of the central charge bounds contained therein.

B. Modular bootstrap

1. Twisted partition functions

The partition function of a unitary, compact, $(1+1)d$ CFT on a spacetime torus encodes the spectrum of scaling dimensions and spins of each primary field of the theory. When the theory has a global, internal symmetry G , we can assign additional quantum numbers accounting for the particular representations ρ of G that states in the Hilbert space of the theory transform in. The torus partition function (which will be denoted pictorially by an empty square with opposite edges identified, i.e., either diagram in Fig. 11 with the trivial TDL in place of \mathcal{L}_g) with modular parameters $\tau, \bar{\tau}$ takes the form (when $c > 1$)

$$Z(\tau, \bar{\tau}) = \text{Tr}(q^{L_0 - \frac{c}{24}} \bar{q}^{\bar{L}_0 - \frac{c}{24}}) \quad (25)$$

$$= \sum_{h, \bar{h}} \sum_{\rho} n_{h, \bar{h}}^{\rho} \chi_{h, \bar{h}}(\tau, \bar{\tau}) \quad (26)$$

where $q = e^{2\pi i \tau}$, $\bar{q} = e^{-2\pi i \bar{\tau}}$, $\chi_{h, \bar{h}}(\tau, \bar{\tau}) = \chi_h(\tau) \bar{\chi}_{\bar{h}}(\bar{\tau})$, and χ_h are the Virasoro characters

$$\chi_0(\tau) = \frac{(1-q)}{\eta(\tau)} q^{-\frac{c-1}{24}}, \quad \chi_h(\tau) = \frac{1}{\eta(\tau)} q^{h - \frac{c-1}{24}},$$

where $\eta(\tau)$ is the Dedekind eta function. Note that to do modular bootstrap calculations, we use so-called reduced characters, defined by replacing $\chi_h(\tau) \rightarrow \tau^{1/4} \eta(q) \chi_h(\tau)$. Henceforth, when we write $\chi_h(\tau)$ etc., we will always be referring to these reduced Virasoro characters. In (26), $n_{h, \bar{h}}^{\rho}$ are positive integers equal to the dimension of the irreducible representation ρ times its multiplicity within each Verma module for conformal dimensions h, \bar{h} . The assumption of compactness ensures that there is a unique ground state and a discrete spectrum when the spatial extent of spacetime is finite. The partition function is constrained to be invariant under $SL(2, \mathbb{Z})$ modular transformations. Such transformations relate descriptions of the same tori with different values of the modular parameters and are generated by the modular S and

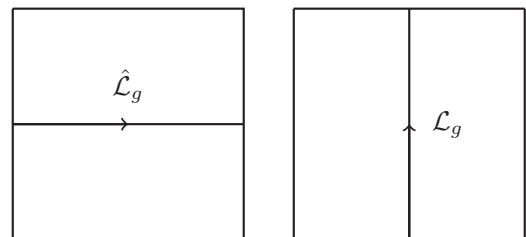


FIG. 11. Each square represents a torus, since opposite edges are identified, where we quantize the theory on horizontal spatial slices. On left is the torus partition with a horizontal twist, corresponding to acting with symmetry across one period of imaginary time evolution. On right is the torus partition function with a vertical twist, corresponding to the partition function of the theory subject to a \mathcal{L}_g -twisted boundary condition.

T transformations

$$S : \tau \rightarrow -1/\tau \quad T : \tau \rightarrow \tau + 1.$$

Imposing equivalence of the torus partition function under such transformations leads to the modular invariance constraints

$$Z(\tau, \bar{\tau}) = Z(-1/\tau, -1/\bar{\tau}) = Z(\tau + 1, \bar{\tau} + 1).$$

We can also use TDLs to construct other partition function-like objects that probe aspects of the G global symmetry, which we will call twisted partition functions. These are constructed by considering the theory on a spacetime torus in the presence of TDLs wrapped around the cycles of the torus. When a TDL corresponding to the group element g is wrapped around a spatial cycle, illustrated in the left diagram within Fig. 11, this corresponds to acting with $\hat{\mathcal{L}}_g$ across one period of imaginary time evolution. Specializing to $G = \mathbb{Z}_N^3$, let us denote the group elements of \mathbb{Z}_N^3 by three-component \mathbb{Z}_N -valued vectors, i.e., $g = (i, j, k)$ for some $i, j, k \in \mathbb{Z}_N$. Similarly, let us denote representations of G , which are all one dimensional, in a similar way but, for differentiation, with square brackets $\rho = [i, j, k]$. Then, a state transforming in a representation ρ of G transforms under g as

$$\hat{\mathcal{L}}_g |\rho\rangle = e^{2\pi i \langle \rho, g \rangle / N} |\rho\rangle$$

where $\langle \rho, g \rangle = ii' + jj' + kk'$ for $g = (i, j, k)$, $\rho = [i', j', k']$. With this, we may express the torus partition function with a horizontal twist as

$$\begin{aligned} Z^g(\tau, \bar{\tau}) &= \text{Tr}_{\mathcal{H}}(\hat{\mathcal{L}}_g q^{L_0 - \frac{c}{24}} \bar{q}^{\bar{L}_0 - \frac{c}{24}}) \\ &= \sum_{h, \bar{h}} \sum_{\rho \in \text{Rep}(G)} n_{h, \bar{h}}^\rho e^{2\pi i \langle \rho, g \rangle / N} \chi_h(\tau) \bar{\chi}_{\bar{h}}(\bar{\tau}). \end{aligned}$$

Likewise, if a g -TDL is wrapped around a cycle in the time direction, illustrated within Fig. 11 on the right, then the resulting twisted partition function represents the partition function of the theory where the trace is taken over the defect Hilbert space \mathcal{H}_g ,

$$Z_g(\tau, \bar{\tau}) = \text{Tr}_{\mathcal{H}_g}(q^{L_0 - \frac{c}{24}} \bar{q}^{\bar{L}_0 - \frac{c}{24}}) = \sum_{h, \bar{h}} n_{h, \bar{h}}^g \chi_{h, \bar{h}}(\tau, \bar{\tau}).$$

The coefficients of the above twisted partition function $n_{h, \bar{h}}^g$ are again positive integers representing the degeneracy of each defect operator with conformal dimensions h, \bar{h} . Of course, as we explained previously, the states in the defect Hilbert space may be dressed with (fractionalized) global symmetry quantum numbers as well, but this fact will not be important for our modular bootstrap calculations.

The twisted partition functions are also subject to modular transformation relations. Covariance under T leads to the spin selection rule (12) [30,31,53]. Since a modular S transformation swaps the two cycles of the torus it interchanges the space and time directions. Thus, we see that

$$Z^g(-1/\tau, -1/\bar{\tau}) = Z_g(\tau, \bar{\tau}), \tag{27}$$

$$Z_g(-1/\tau, -1/\bar{\tau}) = Z^{\bar{g}}(\tau, \bar{\tau}). \tag{28}$$

The defect Hilbert space spectrum is thus completely determined by the local operators of the theory and their symmetry

representations. Now, we can construct a $2|G| - 1$ dimensional vector of twisted partition functions

$$\mathbf{Z}(\tau, \bar{\tau}) = \begin{pmatrix} Z(\tau, \bar{\tau}) \\ Z^g(\tau, \bar{\tau}) \\ \vdots \\ Z_g(\tau, \bar{\tau}) \\ \vdots \end{pmatrix}.$$

This allows us to compactly express the modular transformation relations amongst the twisted partition functions

$$\mathbf{Z}(-1/\tau, -1/\bar{\tau}) = P\mathbf{Z}(\tau, \bar{\tau}) \tag{29}$$

where P is a permutation matrix implementing the relations (27,28) between the components of \mathbf{Z} .

Borrowing terminology from Refs. [30,31], \mathbf{Z} is currently expressed in the *twist basis*, but in order to do bootstrap calculations to obtain bounds, which depend on the symmetry representations it is necessary to write \mathbf{Z} in the *charge basis*, in which positivity is manifest. This is done by performing a discrete Fourier transformation on the partition functions Z^g , leading to partition functions counting the contributions from states transforming in a single representation ρ ,

$$\begin{aligned} Z^\rho(\tau, \bar{\tau}) &= \frac{1}{|G|} \sum_{g \in G} e^{-2\pi i \langle \rho, g \rangle / N} Z^g(\tau, \bar{\tau}) \\ &= \sum_{h, \bar{h}} n_{h, \bar{h}}^\rho \chi_h(\tau) \bar{\chi}_{\bar{h}}(\bar{\tau}). \end{aligned}$$

We remind the reader again that the vertically twisted partition functions Z_g already have a decomposition into Virasoro characters with positive coefficients, so no additional change of basis is needed in those instances. Writing $\mathbf{Z}(\tau, \bar{\tau}) = C\tilde{\mathbf{Z}}(\tau, \bar{\tau})$, where $\tilde{\mathbf{Z}}$ is the twisted partition function in the charge basis and C is a matrix implementing the discrete Fourier transformation, we see that $\tilde{\mathbf{Z}}$ transforms under the modular S transformation as

$$\tilde{\mathbf{Z}}(-1/\tau, -1/\bar{\tau}) = F\tilde{\mathbf{Z}}(\tau, \bar{\tau})$$

where $F = C^{-1}PC$.

There is an additional step that we perform that greatly simplifies our calculations, which is a generalization of the procedure outlined in Ref. [31] for reducing the dimension of the vector of twisted partition functions $\tilde{\mathbf{Z}}$. Given some group G , each outer automorphism $\gamma \in \text{Out}(G)$ will generate a reduced vector partition function where the components consist of summing over the twisted partition functions, in the twist basis, corresponding to TDLs, which lie in equivalence classes under γ . The simplest nontrivial example of this is when $\gamma(g) = g^{-1}$, which pairs each TDL with its orientation reversal, which generates the reduction employed in Ref. [31]. In general, to lose no generality in the bootstrap calculations, one finds the largest subgroup of outer automorphisms, which we will denote $\Gamma \subseteq \text{Out}(G)$, that does not mix TDLs with different \mathbb{Z}_N anomalies and performs the reduction with the outer automorphisms in this subgroup. We will denote the equivalence classes of TDLs that are related to each other by group automorphisms in Γ by $[1], \dots, [n_\Gamma]$. That is, denoting

elements of G by g_n , one finds a reduction matrix

$$r_{mn} = \begin{cases} 1 & g_n \in [m] \\ 0 & \text{else} \end{cases}. \quad (30)$$

The full reduction matrix, in the twist basis, is then given by taking two copies of r_{mn} , where each copy reduces the horizontally/vertically twisted partition functions (note that the copy for the vertically twisted partition functions excludes the redundant first row of r representing the untwisted partition function)

$$R_{mn} = \begin{cases} r_{mn} & 1 \leq m \leq n_\Gamma, 1 \leq n \leq |G| \\ r_{(m-n_\Gamma+1)(n-|G|+1)} & n_\Gamma+1 \leq m \leq 2n_\Gamma-1 \\ 0 & |G|+1 \leq n \leq 2|G|-1 \\ & \text{else} \end{cases}. \quad (31)$$

Finally, in the charge basis we write $\tilde{R} = RC$. Then, defining $\tilde{\mathbf{Z}}_{\text{red}} = \tilde{R}\tilde{\mathbf{Z}}$ we may write the simplified modular covariance equation

$$\tilde{\mathbf{Z}}_{\text{red}}(-1/\tau, -1/\bar{\tau}) = F_{\text{red}}\tilde{\mathbf{Z}}_{\text{red}}(\tau, \bar{\tau}) \quad (32)$$

where $F_{\text{red}} = \tilde{R}F\tilde{R}^T(\tilde{R}\tilde{R}^T)^{-1}$. We present F_{red} for the groups \mathbb{Z}_N^3 we consider in this paper in Appendix. Finally, we define the vectors

$$[\mathbf{M}_{h,\bar{h}}^j(\tau, \bar{\tau})]_i = \delta_{ij}\chi_{h,\bar{h}}(-1/\tau, -1/\bar{\tau}) - [F_{\text{red}}]_{ij}\chi_{h,\bar{h}}(\tau, \bar{\tau}). \quad (33)$$

Then the statement of modular covariance of the twisted partition function may be expressed as

$$\sum_{j,h,\bar{h}} n_{j,h,\bar{h}}^j \mathbf{M}_{h,\bar{h}}^j(\tau, \bar{\tau}) = 0. \quad (34)$$

2. Bounding the local operator spectrum

To put upper bounds on the scaling dimension of local operators, similarly to correlator bootstrap we aim to show via semidefinite programming that certain assumptions about the spectrum of local and defect operators in a CFT with some global symmetry and anomaly, encoded in the twisted partition functions, lead to a violation of (34). The new ingredients to the standard modular bootstrap program with global symmetries that we introduce are our bounds coming from correlator bootstrap, which allow the more subtle LSM anomaly to enter our final modular bootstrap calculations. We will explain how those bounds lead to nontrivial lower bounds on the scaling dimension of the lightest defect operators, under the assumption of gaps in the spectrum of local operators, and how this can be used to generate universal upper bounds on the scaling dimension of the lightest local operators with various symmetry properties. Incorporating the bounds from correlator bootstrap gives strictly stronger bounds than modular bootstrap alone, and is essential for finding any bound at all on the lightest charged operator when N is odd.

We can make stronger assumptions about the defect operator spectrum due to our previously obtained bounds $\Delta^*(N, \Delta_D)$ and $c^*(N, \Delta_D, \Delta^{\min})$, for reasons we now explain.

As before, let Δ_0^{\min} and Δ_Q^{\min} denote the assumed lower bounds on the scaling dimension of any scalar, local operator that is, respectively, symmetric or charged under \mathbb{Z}_N^3 . Next

define

$$\begin{aligned} \tilde{\Delta}_D^{\text{scal}}(\Delta_0^{\min}, \Delta_Q^{\min}) &\equiv \min \{ \Delta_D : \Delta^*(N, \Delta_D) \\ &\geq \max(\Delta_0^{\min}, \Delta_Q^{\min}) \}. \end{aligned}$$

This represents the minimum scaling dimension of a defect operator living on a nonanomalous, order N TDL whose OPE does not necessarily contain local operators whose scaling dimensions violate the assumed gaps. Thus, $\tilde{\Delta}_D^{\text{scal}}(\Delta_0^{\min}, \Delta_Q^{\min})$ is a lower bound on the scaling dimension of any such defect operator. To incorporate the central charge lower bounds, when $\Delta_0^{\min} = \Delta_Q^{\min} = \Delta^{\min}$, we define

$$\tilde{\Delta}_D^{\text{cent}}(\Delta^{\min}, c) \equiv \min \{ \Delta_D : c^*(N, \Delta_D, \Delta^{\min}) \leq c \},$$

which represents the minimum defect operator scaling dimension consistent with gaps $\Delta_0^{\min}, \Delta_Q^{\min}$ and central charge c . Note that, in practice, we can only compute the curves $c^*(N, \Delta_D, \Delta^{\min})$ for a finite list of values $\{\Delta^{(i)}\}$ for the gap in the local operator spectrum Δ^{\min} . Consequently, we perform an interpolation between the central charge curves to achieve the corresponding curve for values of Δ^{\min} between some $\Delta^{(i)}$ and $\Delta^{(i+1)}$. Given functions $f_i(\Delta_D), f_{i+1}(\Delta_D)$ representing such neighboring curves, we use the interpolation $\tilde{f}_{i,i+1}(\Delta_D)$ given by

$$\begin{aligned} \tilde{f}_{i,i+1}(\Delta_D) &\equiv f_{i,i+1}^{-1}(\Delta_D) \\ f_{i,i+1}(c) &\equiv (1-x)f_i^{-1}(c) + xf_{i+1}^{-1}(c) \\ x &\equiv \frac{\Delta^{\min} - \Delta^{(i)}}{\Delta^{(i+1)} - \Delta^{(i)}}. \end{aligned}$$

This has the effect of smoothing out our bounds but introduces a small degree of nonrigorousness. Our focus in this paper is primarily on showing the existence of a bound and its general, qualitative features, so consequently we do not attempt to quantify the error introduced in this way. However, we should certainly discuss this effect in relation to our claim that $(g_2)_1$ is outside the allowed region in our $N = 5$ bound on the lightest local scalar. We can safely rule out $c = \frac{14}{5}$ and $\Delta^{\min} = \frac{4}{5}$ since the curve $c^*(5, \Delta_D, \frac{4}{5})$ is computed exactly, up to discretization effects in Δ_D that should be very small as the curves are quite smooth.

At this point we see that there are two, independent lower bounds on the defect operator scaling dimension that are consistent with either the gaps $\Delta_0^{\min}, \Delta_Q^{\min}$ or the central charge c ; a theory with a defect operator of a lower scaling dimension than the maximum of the two would thus be inconsistent. Finally we define

$$\Delta_D^{\min}(\Delta_0^{\min}, \Delta_Q^{\min}, c) \equiv \max \{ \tilde{\Delta}_D^{\text{scal}}, \tilde{\Delta}_D^{\text{cent}} \}$$

and conclude that this is the lowest possible value of the defect operator scaling dimension consistent with the gaps $\Delta_0^{\min}, \Delta_Q^{\min}$, and c .

The final step is to do a standard modular bootstrap calculation to determine whether the gaps in the local operator spectrum and the gap in the defect operator spectrum are inconsistent with modular covariance of the twisted partition function. To do this, we seek a linear functional, which acts on vector-valued functions of the modular parameters, of the

form

$$\alpha[\mathbf{M}(\tau, \bar{\tau})] = \sum_j \sum_{\substack{m,n=0 \\ m+n \leq \Lambda^{\text{mod}}}}^{\Lambda^{\text{mod}}} a_{mn}^j \partial_\tau^m \partial_{\bar{\tau}}^n [\mathbf{M}(\tau, \bar{\tau})]_j \Big|_{\tau=i, \bar{\tau}=-i} \quad (35)$$

where Λ^{mod} is the modular bootstrap derivative order. In our setup, we will allow primary operators of three different types to enter the spectrum of the theories we consider: the vacuum primary with $h = \bar{h} = 0$, degenerate primaries with either h or \bar{h} being equal to 0, and nondegenerate primaries with $h, \bar{h} > 0$. For the case of degenerate primaries and the vacuum, the degenerate Virasoro character of weight 0 enters, while in the nondegenerate case only the nondegenerate characters enter. Further, we will assume that the spectrum of the theories we consider is parity invariant, meaning $n_{h,\bar{h}}^j = n_{\bar{h},h}^j$ without loss of generality, since the anomalies considered in this paper are compatible with such an assumption [30,31,102]. We thus will define

$$\mathbf{M}_{\Delta,s}^j(\tau, \bar{\tau}) \equiv \mathbf{M}_{h,\bar{h}}^j(\tau, \bar{\tau}) + \mathbf{M}_{\bar{h},h}^j(\tau, \bar{\tau})$$

where $\Delta = h + \bar{h}$, $s = h - \bar{h}$ and we assume $s \geq 0$. Note that, in this notation, we can denote the contribution from degenerate Virasoro primaries (including that of the vacuum) by $\mathbf{M}_{s,s}^j(\tau, \bar{\tau})$ for $s > 0$. The linear functional (35) that we search for will be constrained to have the following properties:

$$\begin{aligned} \alpha[\mathbf{M}_{0,0}^1] &= 1 \\ \alpha[\mathbf{M}_{\Delta,s}^i] &\geq 0 \quad \forall \Delta \geq \begin{cases} \Delta_0^{\min} & i = 1, & s = 0 \\ \Delta_Q^{\min} & 2 \leq i \leq n_\gamma, & s = 0 \\ \Delta_D^{\min} & i = 2n_\gamma - 1, & s = 0 \\ |s| & \text{else,} & s \leq S_{\max}^{\text{mod}} \in S_i \end{cases} \\ \alpha[\mathbf{M}_{s,s}^i] &\geq 0 \quad \forall s \leq S_{\max}^{\text{mod}} \in S_i \end{aligned}$$

where we use S_i to denote the spins allowed by the spin selection rule for the local operators, which are just any integer, and defect operators, given in Table I, for the i th composite sector. Note that $2n_\gamma - 1$ is the index denoting the composite defect sector corresponding to nonanomalous, order N TDLs. Further we denote our spin truncation parameter for our modular bootstrap calculations by S_{\max}^{mod} .

Upon finding such a linear functional α , we conclude that the assumed gaps Δ_0^{\min} and Δ_Q^{\min} are inconsistent with both modular covariance of the twisted partition function and crossing symmetry of defect operators. When we successfully find a linear functional obeying the constraints when $\Delta_0^{\min} = 0$ this represents an upper bound on the lightest charged operator, and similarly when $\Delta_0^{\min} = \Delta_Q^{\min}$ we get a bound on the lightest local operator. Either of these bounds may be optimized, to within a small numerical tolerance, to obtain the final bounds, which are shown in Fig. 2. This concludes our description of our modifications to the usual modular bootstrap procedure.

V. CONCLUSIONS

In this paper, we take an additional step towards constraining the space of $(1+1)d$ bosonic CFTs with finite global

symmetries and anomalies. To this end, we incorporate a more complete picture of the symmetry properties of defect operators into the modular bootstrap, exploiting the delicate balance between the spectrum of defect operators and local operators. We make the relationship between the spectra of defect and local operators quantitatively precise using conformal bootstrap techniques, and in the end obtain universal bounds on the spectrum of local operators. Our primary result is a generalization of the main results of Refs. [30,31] that \mathbb{Z}_N anomalies imply the presence of light, charged operators in a CFT. What we show is that this statement continues to hold for a class of \mathbb{Z}_N^3 anomalies that, in some cases, do not lead to any nontrivial spin selection rule for certain defect operators. The particular symmetries and anomalies that we study occur in physically relevant situations such as spin chains obeying LSM-type constraints, and in somewhat more fine-tuned situations such as multicritical points of $(1+1)d$ SPT phases. Of course, our bounds also apply to the gapless boundary theories of in-cohomology $(2+1)d$ SPT phases protected by \mathbb{Z}_N^3 symmetry with 3-cocycle ω given by (14).

A question that motivated this paper is how, if at all, the central charge of a $(1+1)d$ CFT is bounded from below by its discrete symmetries and anomalies. As far as symmetry goes, it is known that a CFT with a finite global symmetry whose faithfully realized part is a group larger than \mathbb{Z}_2 or S_3 must have $c \geq 1$ [54]. Further, the Sugawara construction provides a formula for the minimum central charge needed to accommodate continuous global symmetries, which is generally even larger than $c = 1$ [37]. Thus, restricting to general finite symmetries, we are interested in the question of whether any lower bound $c > 1$ can be proven when the symmetry is anomalous.

Consequently, another goal of our paper was to search for numerical bootstrap evidence that could test whether certain suggested lower bounds are reasonable. Some of our calculations seem to suggest that existing, proposed bounds are not quantitatively correct. Specifically, in the case $N = 5$ that we study, there is a prominent kink in our plot, but it does not obviously correspond to any known theory. The location of the kink is nearly coincident with the WZW CFT $(g_2)_1$, which has central charge $c = 14/5$, but upon doing more careful numerics we were able to place this theory outside of the allowed region. Since bootstrap calculations can only rigorously show what is disallowed, it is difficult to make any statements about features in the allowed region when they do not appear to correspond to known theories. In the future, it will be interesting to explore more carefully the region near this kink to look for other signatures that can explain the kink as an actual theory. We expect that using a mixed correlator bootstrap setup will especially help in this direction, which we are actively investigating. More generally, we are hopeful that future analysis, guided by the evidence provided here, together with additional analytic or numerical calculations, will produce the types of central charge bounds that we desire.

There are various exciting avenues for future study that we would like to mention. First, we can consider technical improvements to the calculations that were done in this paper. Among them are, first, using Virasoro conformal blocks for the correlator bootstrap constraints; this would quantitatively improve the bounds and is also a way to directly incorporate

the central charge into the correlator bootstrap calculations without needing to assume a nongeneric gap in the spectrum of symmetric local operators. Second, we think it would be very interesting to consider the problem of bootstrapping correlation functions of defect operators with fractional spin, which could produce bootstrap bounds on defect operators in the most general setting. The aforementioned improvements would open up the possibility of obtaining current state-of-the-art universal bounds for completely general finite global symmetries and anomalies. This seems especially interesting when the symmetry is described by a fusion category with some noninvertible TDLs. There are countless examples of interesting theories with such noninvertible symmetries, especially in the context of $(1 + 1)d$ CFT, so exploring the space of CFTs with such symmetries using bootstrap is a natural future direction. This story has been initiated in [103], and we expect more general cases to be improved by the techniques introduced in this paper.

Generalizations of our story to CFTs in higher dimensions seem especially interesting, albeit seemingly in the absence of a useful analog of modular invariance [104]. Some progress in this direction has been made already [105], but accounting for the complete picture of symmetries [106] and anomalies in higher dimensions within bootstrap remains a challenge. There is significant condensed matter theory motivation to incorporate anomalies into bootstrap, since, for instance, it could provide another way to explore the properties of exotic gapless states (see [107,108]).

How might such higher-dimensional generalizations be achieved? In $(1 + 1)d$, there is a clear relationship between defect operators and local operators since both sets of operators contribute to the twisted torus partition function, and the OPE of defect operators may contain local operators. In contrast, defect operators corresponding to 0-form global symmetries in dimensions $d + 1 > 2$ are extended objects, given by conformal defects attached to codimension-1 topological hypersurfaces (for example, in the $3d$ Ising CFT an example of this is the disorder operator, sometimes known as the twist defect). Such conformal defects host localized operators that have reduced conformal symmetry. Perhaps, then, the implications of anomalies can be reduced to some properties of these operators. There has been much study of such extended objects using a wide range of techniques [109,110], including via conformal field theory techniques and bootstrap [111–113], so including anomalies into the story seems like a natural next step. There are, however, some technical issues that seem to prohibit the most direct generalizations of our paper to cases involving extended defects—see Ref. [114]. Additionally, as already pointed out in Ref. [30], anomalies of finite 0-form symmetries in bosonic CFTs in dimensions $d + 1 > 2$ can be saturated by gapped topological theories, which have a unique ground state on the spatial sphere. This eliminates the possibility that such anomalies can lead to refined bounds on the spectrum of local operators since any CFT can be made to have any anomaly in this class via stacking gapped degrees of freedom. For such anomalies, it then seems that the questions that bootstrap may be able to answer are those concerning the properties of the extended defects. However, there are several classes of anomalies that ensure gaplessness in higher dimensions, including anomalies

for continuous symmetries and even cases involving discrete symmetries [22,115]. It thus seems promising to continue to develop new ways to incorporate the constraints of such symmetries and anomalies into bootstrap.

ACKNOWLEDGMENTS

This work was facilitated through the use of advanced computational, storage, and networking infrastructure provided by the Hyak supercomputer system and funded by the Student Technology Fee at the University of Washington. We thank Tyler Ellison, Justin Kaidi, Ho Tat Lam, Sahand Seifnashri, Shu-Heng Shao, and Nathanan Tantivasadakarn for helpful discussions. We especially thank Tyler Ellison, Justin Kaidi, and Shu-Heng Shao for comments on an initial draft of this paper. We thank Mocho Go and Yuji Tachikawa for their assistance with `autoboot`. R.L. thanks the 2021 annual meeting for the Simons Collaboration on Non-Perturbative bootstrap, as well as the Simons Center for Geometry and Physics at Stony Brook University, for hospitality. R.L. and L.F. are supported by NSF Grant No. DMR-1939864.

APPENDIX: MODULAR BOOTSTRAP EQUATIONS

The reduced modular covariance equation reads

$$\tilde{Z}_{\text{red}}(-1/\tau, -1/\bar{\tau}) = F_{\text{red}} \tilde{Z}_{\text{red}}(\tau, \bar{\tau}).$$

Here we list F_{ref} for each N along with the corresponding reduced partition function components.

1. $N \in 2\mathbb{Z} + 1$

As discussed, when N is odd the LSM anomaly does not lead any \mathbb{Z}_N subgroup to have a \mathbb{Z}_N anomaly. When N is prime, such as in the cases we consider, the full orbit of the automorphism group of any nontrivial $g \in \mathbb{Z}_N^3$ contains all other nontrivial TDLs. Consequently, we may perform the maximal reduction and lose no generality. If we denote the trivial representation by ρ_1 and the trivial element of G by g_1 then

$$F_{\text{red}} = \begin{pmatrix} \frac{1}{|G|} & \frac{1}{|G|} & \frac{1}{|G|} \\ \frac{|G|-1}{|G|} & \frac{|G|-1}{|G|} & -\frac{1}{|G|} \\ |G|-1 & -1 & 0 \end{pmatrix},$$

$$\tilde{Z}_{\text{red}} = \begin{pmatrix} Z^{\rho_1} \\ \sum_{\rho_1 \neq \rho \in \text{Rep}(G)} Z^\rho \\ \sum_{g_1 \neq g \in G} Z_g \end{pmatrix}.$$

2. $N \in 2\mathbb{Z}$

In the case of even N , the full reduction is no longer possible. However, by grouping together all TDLs with identical \mathbb{Z}_M anomalies according to Table I we still may perform a nontrivial reduction.

a. $N = 2$

According to Table I there are two types of TDLs, both with order 2: nonanomalous or anomalous with $k = 1$. Denote

the subset of G corresponding to the former as [2N] and the latter as [2A].

Next, denote representations of \mathbb{Z}_N^3 as vectors $\rho = [i, j, k]$. There are then two automorphism classes of representations induced by automorphisms preserving the spin selection rules of the LSM anomaly: a class [O] where an odd number of components of ρ is nontrivial and a class [E] where an even number is nontrivial. Then

$$F_{\text{red}} = \begin{pmatrix} \frac{1}{8} & \frac{1}{8} & \frac{1}{8} & \frac{1}{8} & \frac{1}{8} \\ \frac{3}{8} & \frac{3}{8} & \frac{3}{8} & \frac{3}{8} & -\frac{1}{8} \\ \frac{1}{2} & \frac{1}{2} & \frac{1}{2} & -\frac{1}{2} & 0 \\ 1 & 1 & -1 & 0 & 0 \\ 6 & -2 & 0 & 0 & 0 \end{pmatrix}, \quad \tilde{Z}_{\text{red}} = \begin{pmatrix} Z^{\rho_1} \\ \sum_{\rho \in [E]} Z^\rho \\ \sum_{\rho \in [O]} Z^\rho \\ \sum_{g \in [2A]} Z_g \\ \sum_{g \in [2N]} Z_g \end{pmatrix}.$$

$$F_{\text{red}} = \begin{pmatrix} \frac{1}{64} & \frac{1}{64} & \frac{1}{64} & \frac{1}{64} & \frac{1}{64} & \frac{1}{64} & \frac{1}{64} \\ \frac{3}{64} & \frac{3}{64} & \frac{3}{64} & \frac{3}{64} & \frac{3}{64} & \frac{3}{64} & -\frac{1}{64} \\ \frac{1}{16} & \frac{1}{16} & \frac{1}{16} & \frac{1}{16} & \frac{1}{16} & -\frac{1}{16} & 0 \\ \frac{7}{8} & \frac{7}{8} & \frac{7}{8} & \frac{7}{8} & -\frac{1}{8} & 0 & 0 \\ 7 & 7 & 7 & -1 & 0 & 0 & 0 \\ 8 & 8 & -8 & 0 & 0 & 0 & 0 \\ 48 & -16 & 0 & 0 & 0 & 0 & 0 \end{pmatrix}, \quad \tilde{Z}_{\text{red}} = \begin{pmatrix} Z^{\rho_1} \\ \sum_{\rho \in [2E]} Z^\rho \\ \sum_{\rho \in [2O]} Z^\rho \\ \sum_{\rho \in [4]} Z^\rho \\ \sum_{g \in [2N]} Z_g \\ \sum_{g \in [4A]} Z_g \\ \sum_{g \in [4N]} Z_g \end{pmatrix}.$$

c. $N = 6$

Following a similar pattern as before, we label the classes of TDLs as [2N], [2A], [3N], [6N], [6A] where the order 2 anomalous TDLs have $k = 1$ and the order 6 anomalous TDLs have $k = 3$. There are five classes of nontrivial representations. We denote the classes containing an even/odd number of components being equal to 3 as [3E]/[3O]. There is a class where each component is an even number, which we denote by [E]. There is a class containing only odd numbers with at least one component not equal to 3, denoted [O]. Finally, there is a class where the components are a mix of even and odd numbers, denoted [EO]. These give

$$F_{\text{red}} = \begin{pmatrix} \frac{1}{216} & \frac{1}{216} \\ \frac{1}{72} & -\frac{1}{216} & \frac{1}{72} & \frac{1}{72} & -\frac{1}{216} \\ \frac{1}{54} & \frac{1}{54} & \frac{1}{54} & \frac{1}{54} & \frac{1}{54} & \frac{1}{54} & -\frac{1}{54} & 0 & \frac{1}{54} & -\frac{1}{54} & 0 \\ \frac{13}{108} & -\frac{1}{216} & -\frac{1}{216} & -\frac{1}{216} \\ \frac{13}{36} & -\frac{13}{108} & -\frac{1}{72} & -\frac{1}{72} & \frac{1}{216} \\ \frac{13}{27} & \frac{13}{27} & \frac{13}{27} & \frac{13}{27} & \frac{13}{27} & \frac{13}{27} & -\frac{13}{27} & 0 & -\frac{1}{54} & -\frac{1}{54} & 0 \\ 1 & 1 & -1 & 1 & 1 & -1 & 0 & 0 & 0 & 0 & 0 \\ 6 & -2 & 0 & 6 & -2 & 0 & 0 & 0 & 0 & 0 & 0 \\ 26 & 26 & 26 & -1 & -1 & -1 & 0 & 0 & 0 & 0 & 0 \\ 26 & 26 & -26 & -1 & -1 & 1 & 0 & 0 & 0 & 0 & 0 \\ 156 & -52 & 0 & -6 & 2 & 0 & 0 & 0 & 0 & 0 & 0 \end{pmatrix}, \quad \tilde{Z}_{\text{red}} = \begin{pmatrix} Z^{\rho_1} \\ \sum_{\rho \in [3E]} Z^\rho \\ \sum_{\rho \in [3O]} Z^\rho \\ \sum_{\rho \in [E]} Z^\rho \\ \sum_{\rho \in [O]} Z^\rho \\ \sum_{\rho \in [EO]} Z^\rho \\ \sum_{g \in [2A]} Z_g \\ \sum_{g \in [2N]} Z_g \\ \sum_{g \in [3N]} Z_g \\ \sum_{g \in [6A]} Z_g \\ \sum_{g \in [6N]} Z_g \end{pmatrix}.$$

- [1] E. H. Lieb, T. Schultz, and D. Mattis, *Ann. Phys.* **16**, 407 (1961).
 [2] F. D. M. Haldane, *Phys. Rev. Lett.* **50**, 1153 (1983).
 [3] I. Affleck and E. H. Lieb, *Lett. Math. Phys.* **12**, 57 (1986).
 [4] M. Oshikawa, *Phys. Rev. Lett.* **84**, 1535 (2000).
 [5] M. B. Hastings, *Phys. Rev. B* **69**, 104431 (2004).
 [6] S. A. Parameswaran, A. M. Turner, D. P. Arovas, and A. Vishwanath, *Nat. Phys.* **9**, 299 (2013).
 [7] H. Watanabe, H. C. Po, A. Vishwanath, and M. Zaletel, *Proc. Natl. Acad. Sci. USA* **112**, 14551 (2015).
 [8] S.-J. Huang, H. Song, Y.-P. Huang, and M. Hermele, *Phys. Rev. B* **96**, 205106 (2017).
 [9] D. V. Else and R. Thorngren, *Phys. Rev. B* **101**, 224437 (2020).
 [10] M. Cheng, *Phys. Rev. B* **99**, 075143 (2019).
 [11] Y.-M. Lu, *arXiv:1705.04691*.
 [12] X. Yang, S. Jiang, A. Vishwanath, and Y. Ran, *Phys. Rev. B* **98**, 125120 (2018).
 [13] R. Kobayashi, K. Shiozaki, Y. Kikuchi, and S. Ryu, *Phys. Rev. B* **99**, 014402 (2019).

- [14] X. Chen, Z.-C. Gu, and X.-G. Wen, *Phys. Rev. B* **83**, 035107 (2011).
- [15] Y. Ogata and H. Tasaki, *Commun. Math. Phys.* **372**, 951 (2019).
- [16] Y. Ogata, Y. Tachikawa, and H. Tasaki, *Commun. Math. Phys.* **385**, 79 (2021).
- [17] A. Prakash, [arXiv:2002.11176](https://arxiv.org/abs/2002.11176).
- [18] S. C. Furuya and M. Oshikawa, *Phys. Rev. Lett.* **118**, 021601 (2017).
- [19] M. Cheng, M. Zaletel, M. Barkeshli, A. Vishwanath, and P. Bonderson, *Phys. Rev. X* **6**, 041068 (2016).
- [20] G. Y. Cho, C.-T. Hsieh, and S. Ryu, *Phys. Rev. B* **96**, 195105 (2017).
- [21] M. Metlitski and R. Thorngren, *Phys. Rev. B* **98**, 085140 (2018).
- [22] C. Córdova and K. Ohmori, [arXiv:1910.04962](https://arxiv.org/abs/1910.04962).
- [23] G. Hooft, in *Recent Developments in Gauge Theories*, edited by G. Hooft, C. Itzykson, A. Jaffe, H. Lehmann, P. K. Mitter, I. M. Singer, and R. Stora (Springer US, Boston, 1980), pp. 135–157.
- [24] X. Chen and X.-G. Wen, *Phys. Rev. B* **86**, 235135 (2012).
- [25] L. H. Santos and J. Wang, *Phys. Rev. B* **89**, 195122 (2014).
- [26] J. C. Wang, L. H. Santos, and X.-G. Wen, *Phys. Rev. B* **91**, 195134 (2015).
- [27] J. C. Bridgeman and D. J. Williamson, *Phys. Rev. B* **96**, 125104 (2017).
- [28] M. Cheng and N. Seiberg, [arXiv:2211.12543](https://arxiv.org/abs/2211.12543).
- [29] Y. Alavirad and M. Barkeshli, *Phys. Rev. B* **104**, 045151 (2021).
- [30] Y.-H. Lin and S.-H. Shao, *Phys. Rev. D* **100**, 025013 (2019).
- [31] Y.-H. Lin and S.-H. Shao, *Phys. Rev. D* **103**, 125001 (2021).
- [32] A. B. Zamolodchikov, *JETP Lett.* **43**, 565 (1986).
- [33] J. Polchinski, *Nucl. Phys. B* **303**, 226 (1988).
- [34] J. Cardy, *Scaling and Renormalization in Statistical Physics*, Cambridge Lecture Notes in Physics (Cambridge University Press, Cambridge, 1996).
- [35] Y. Nakayama, [arXiv:1302.0884](https://arxiv.org/abs/1302.0884).
- [36] M. Cheng and D. J. Williamson, *Phys. Rev. Res.* **2**, 043044 (2020).
- [37] P. Di Francesco, P. Mathieu, and D. Sénéchal, *Conformal Field Theory*, Graduate Texts in Contemporary Physics (Springer, New York, 1997).
- [38] A. Belavin, A. Polyakov, and A. Zamolodchikov, *Nucl. Phys. B* **241**, 333 (1984).
- [39] D. Friedan, Z. Qiu, and S. Shenker, *Phys. Rev. Lett.* **52**, 1575 (1984).
- [40] G. Moore and N. Seiberg, *Commun. Math. Phys.* **123**, 177 (1989).
- [41] R. Rattazzi, V. S. Rychkov, E. Tonni, and A. Vichi, *J. High Energy Phys.* **12** (2008) 031.
- [42] S. El-Showk, M. F. Paulos, D. Poland, S. Rychkov, D. Simmons-Duffin, and A. Vichi, *Phys. Rev. D* **86**, 025022 (2012).
- [43] D. Poland, S. Rychkov, and A. Vichi, *Rev. Mod. Phys.* **91**, 015002 (2019).
- [44] S. El-Showk, M. F. Paulos, D. Poland, S. Rychkov, D. Simmons-Duffin, and A. Vichi, *J. Stat. Phys.* **157**, 869 (2014).
- [45] D. Simmons-Duffin, *J. High Energy Phys.* **03** (2017) 086.
- [46] D. Simmons-Duffin, *J. High Energy Phys.* **06** (2015) 174.
- [47] S. Hellerman, *J. High Energy Phys.* **08** (2011) 130.
- [48] S. Collier, Y.-H. Lin, and X. Yin, *J. High Energy Phys.* **09** (2018) 061.
- [49] Actually, in general dimensions $d + 1 > 2$ there are ways to put universal bounds on the local operator spectrum. Most generally, every unitary CFT possesses a conserved stress tensor, so it may be used as an external field in correlator bootstrap calculations and the content of its OPE with itself may be studied, leading to universal bounds on the lightest operator [116]. However, it is not possible to obtain universal bounds in this way that are refined by discrete, internal symmetries since the stress tensor does not interact nontrivially with such symmetries. For continuous internal symmetries, a similar approach may be used to obtain universal bounds by using the conserved currents of the symmetry [117].
- [50] N. Benjamin and Y.-H. Lin, *SciPost Phys. Proc.* **9**, 065 (2020).
- [51] A. Grigoletto and P. Putrov, [arXiv:2106.16247](https://arxiv.org/abs/2106.16247).
- [52] A. Grigoletto, [arXiv:2112.01485](https://arxiv.org/abs/2112.01485).
- [53] C.-M. Chang, Y.-H. Lin, S.-H. Shao, Y. Wang, and X. Yin, *J. High Energy Phys.* **01** (2019) 026.
- [54] P. Ruelle and O. Verhoeven, *Nucl. Phys. B* **535**, 650 (1998).
- [55] N. Afkhami-Jeddi, H. Cohn, T. Hartman, and A. Tajdini, *J. High Energy Phys.* **01** (2021) 130.
- [56] N. Angelinos, D. Chakraborty, and A. Dymarsky, *J. High Energy Phys.* **11** (2022) 118.
- [57] N. Benjamin, S. Collier, A. L. Fitzpatrick, A. Maloney, and E. Perlmutter, *J. High Energy Phys.* **09** (2021) 174.
- [58] A. Dymarsky and A. Shapere, *J. High Energy Phys.* **03** (2021) 160.
- [59] X. Chen, Z.-C. Gu, and X.-G. Wen, *Phys. Rev. B* **82**, 155138 (2010).
- [60] X. Chen, Z.-C. Gu, Z.-X. Liu, and X.-G. Wen, *Phys. Rev. B* **87**, 155114 (2013).
- [61] L. Tsui, H.-C. Jiang, Y.-M. Lu, and D.-H. Lee, *Nucl. Phys. B* **896**, 330 (2015).
- [62] L. Tsui, Y.-T. Huang, H.-C. Jiang, and D.-H. Lee, *Nucl. Phys. B* **919**, 470 (2017).
- [63] R. Verresen, R. Moessner, and F. Pollmann, *Phys. Rev. B* **96**, 165124 (2017).
- [64] L. Tsui, Y.-T. Huang, and D.-H. Lee, *Nucl. Phys. B* **949**, 114799 (2019).
- [65] N. Bultinck, *Phys. Rev. B* **100**, 165132 (2019).
- [66] N. Tantivasadakarn, R. Thorngren, A. Vishwanath, and R. Verresen, *SciPost Phys.* **14**, 012 (2023).
- [67] N. Tantivasadakarn, R. Thorngren, A. Vishwanath, and R. Verresen, *SciPost Phys.* **14**, 013 (2023).
- [68] D. V. Else and C. Nayak, *Phys. Rev. B* **90**, 235137 (2014).
- [69] R. Thorngren and D. V. Else, *Phys. Rev. X* **8**, 011040 (2018).
- [70] W. Ye, M. Guo, Y.-C. He, C. Wang, and L. Zou, *SciPost Phys.* **13**, 066 (2022).
- [71] M. Oshikawa and I. Affleck, *Phys. Rev. Lett.* **77**, 2604 (1996).
- [72] M. Oshikawa and I. Affleck, *Nucl. Phys. B* **495**, 533 (1997).
- [73] V. B. Petkova and J. B. Zuber, *Phys. Lett. B* **504**, 157 (2001).
- [74] J. Fröhlich, J. Fuchs, I. Runkel, and C. Schweigert, *Phys. Rev. Lett.* **93**, 070601 (2004).
- [75] A. Kitaev, *Ann. Phys.* **321**, 2 (2006).
- [76] J. Fröhlich, J. Fuchs, I. Runkel, and C. Schweigert, *Nucl. Phys. B* **763**, 354 (2007).

- [77] D. Gaiotto, A. Kapustin, N. Seiberg, and B. Willett, *J. High Energy Phys.* **02** (2015) 172.
- [78] P. Etingof, S. Gelaki, D. Nikshych, and V. Ostrik, *Tensor Categories* (American Mathematical Society, Providence, RI, 2015).
- [79] T. Quella, I. Runkel, and G. M. T. Watts, *J. High Energy Phys.* **04** (2007) 095.
- [80] C. Vafa and E. Witten, *J. Geom. Phys.* **15**, 189 (1995).
- [81] R. Dijkgraaf and E. Witten, *Commun. Math. Phys.* **129**, 393 (1990).
- [82] C. Wang and M. Levin, *Phys. Rev. B* **91**, 165119 (2015).
- [83] R. Verresen, R. Thorngren, N. G. Jones, and F. Pollmann, *Phys. Rev. X* **11**, 041059 (2021).
- [84] M. d. W. Propitius, [arXiv:hep-th/9511195](https://arxiv.org/abs/hep-th/9511195).
- [85] A. Tiwari, X. Chen, K. Shiozaki, and S. Ryu, *Phys. Rev. B* **97**, 245133 (2018).
- [86] D. Robbins and T. Vandermeulen, *Phys. Rev. D* **101**, 106021 (2020).
- [87] We thank Sahand Seifnashri and especially Shu-Heng Shao for helpful conversations and suggestions related to the content in this section.
- [88] C. Vafa, *Nucl. Phys. B* **273**, 592 (1986).
- [89] Y. Tachikawa, *SciPost Phys.* **8**, 015 (2020).
- [90] L. Bhardwaj and Y. Tachikawa, *J. High Energy Phys.* **03** (2018) 189.
- [91] R. Thorngren and Y. Wang, [arXiv:1912.02817](https://arxiv.org/abs/1912.02817).
- [92] D. Gaiotto, A. Kapustin, Z. Komargodski, and N. Seiberg, *J. High Energy Phys.* **05** (2017) 091.
- [93] GAP, GAP–Groups, Algorithms, and Programming, Version 4.11.1, The GAP Group (2021).
- [94] C.-M. Chang and Y.-H. Lin, *J. High Energy Phys.* **10** (2021) 125.
- [95] T.-C. Huang, Y.-H. Lin, and S. Seifnashri, *J. High Energy Phys.* **12** (2021) 028.
- [96] M. Go and Y. Tachikawa, *J. High Energy Phys.* **06** (2019) 084.
- [97] We thank Mocho Go and Yuji Tachikawa for their time in assisting us in setting up autoboot and finding a bug that prevented our correlator bootstrap calculations from working.
- [98] H. Osborn, *Phys. Lett. B* **718**, 169 (2012).
- [99] S. M. Chester, [arXiv:1907.05147](https://arxiv.org/abs/1907.05147).
- [100] Note that the extra factor of $\sqrt{\dim R}$ arises due to the definition in autoboot of the OPE coefficient $\lambda_{\phi\phi_I} = \sqrt{\dim R}$ for an operator ϕ transforming in the representation R of the internal symmetry.
- [101] A. Vichi, *EPFL*, 181 (2011).
- [102] T. Anous, R. Mahajan, and E. Shaghoulian, *SciPost Phys.* **5**, 022 (2018).
- [103] Y.-H. Lin and S.-H. Shao, [arXiv:2302.13900](https://arxiv.org/abs/2302.13900).
- [104] A. Belin, J. de Boer, and J. Kruthoff, *SciPost Phys.* **5**, 060 (2018).
- [105] Y.-H. Lin, D. Meltzer, S.-H. Shao, and A. Stergiou, *Phys. Rev. D* **101**, 125007 (2020).
- [106] Symmetry in QFT in higher dimensions is an active area of study. See Refs. [77,118–120] for recent progress.
- [107] L. Zou, Y.-C. He, and C. Wang, *Phys. Rev. X* **11**, 031043 (2021).
- [108] Y.-C. He, J. Rong, and N. Su, *SciPost Phys.* **13**, 014 (2022).
- [109] Y.-C. Wang, M. Cheng, and Z. Y. Meng, *Phys. Rev. B* **104**, L081109 (2021).
- [110] Y.-C. Wang, N. Ma, M. Cheng, and Z. Y. Meng, *SciPost Phys.* **13**, 123 (2022).
- [111] M. Billó, M. Caselle, D. Gaiotto, F. Gliozzi, M. Meineri, and R. Pellegrini, Line defects in the 3D Ising model (2013).
- [112] D. Gaiotto, D. Mazac, and M. F. Paulos, *J. High Energy Phys.* **03** (2014) 100.
- [113] M. Billó, V. Gonçalves, E. Lauria, and M. Meineri, *J. High Energy Phys.* **04** (2016) 091.
- [114] A. Söderberg, *J. High Energy Phys.* **04** (2021) 087.
- [115] C. Córdova and K. Ohmori, *Phys. Rev. D* **102**, 025011 (2020).
- [116] A. Dymarsky, F. Kos, P. Kravchuk, D. Poland, and D. Simmons-Duffin, *J. High Energy Phys.* **02** (2018) 164.
- [117] A. Dymarsky, J. Penedones, E. Trevisani, and A. Vichi, *J. High Energy Phys.* **05** (2019) 098.
- [118] C. Córdova, T. T. Dumitrescu, and K. Intriligator, *J. High Energy Phys.* **02** (2019) 184.
- [119] F. Benini, C. Córdova, and P.-S. Hsin, *J. High Energy Phys.* **03** (2019) 118.
- [120] L. Bhardwaj, L. Bottini, S. Schafer-Nameki, and A. Tiwari, *SciPost Phys.* **14**, 007 (2023).